Potential Oncogenicity of Synthetic mRNA Vaccines: Convergent Mechanistic, Clinical, and Population Evidence for a Concurrent-Hit Model of Accelerated Malignancy

John A. Catanzaro, NMD, PhD[1], Nicolas Hulscher, MPH[2]*, Raphael B. Stricker, MD[3], Jamie K. Waselenko, MD, FACP, FICT[4], Peter A. McCullough, MD, MPH[2]

[1]Neo7Bioscience, Inc, Dallas, TX

[2]McCullough Foundation, Dallas, TX

[3]Union Square Medical Associates, San Francisco, CA

[4]Cincinnati Integrative Oncology and Functional Medicine, Cincinnati, OH

***Correspondence**: nichulscher@gmail.com

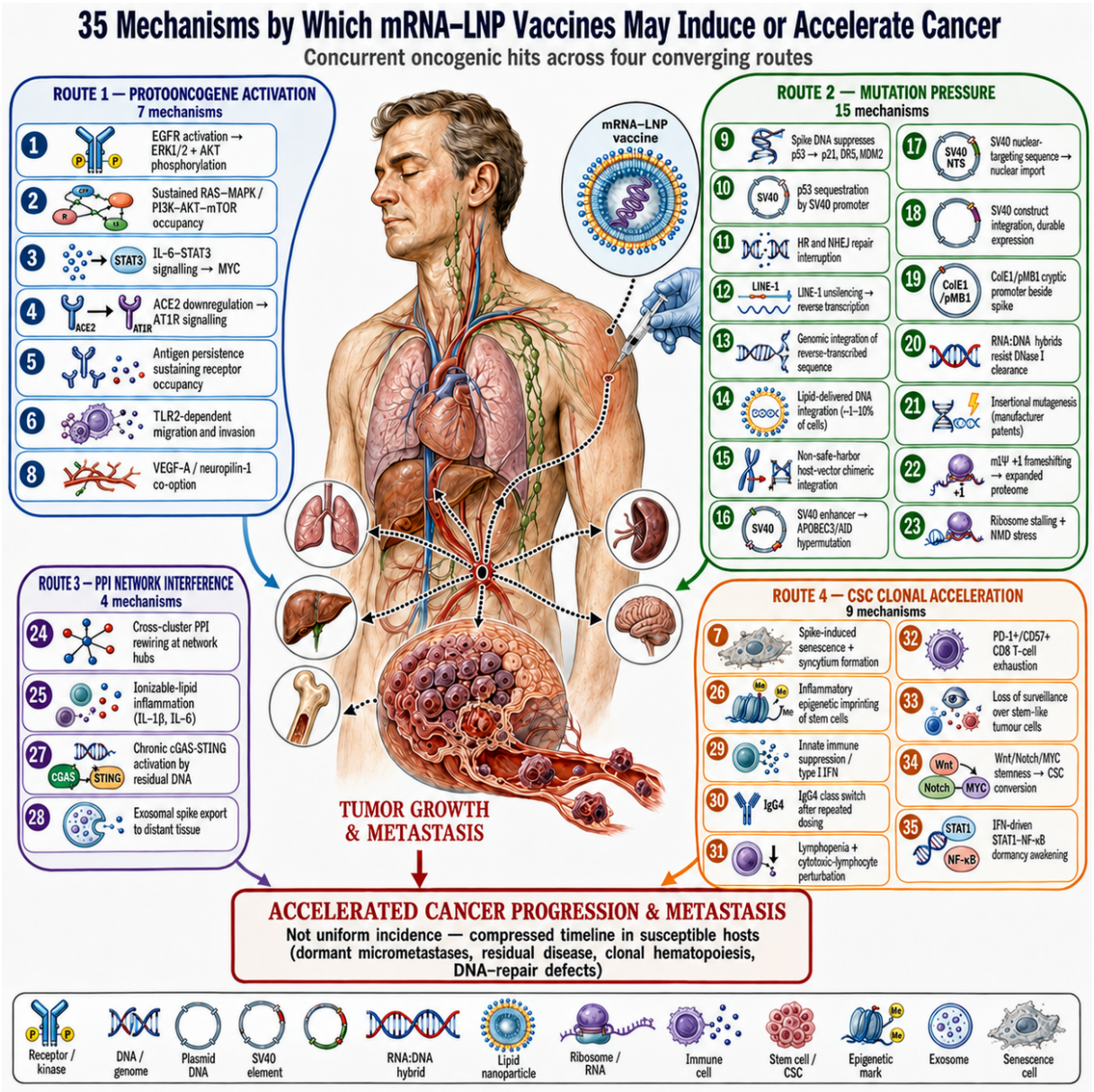

Abstract

Cancer commonly has mechanistically diverse features—sustained proliferative signaling, evasion of growth suppression and death, genomic instability, inflammation, immune evasion, and stem-like plasticity—capabilities that ordinarily assemble over years. Nucleoside-modified mRNA–lipid nanoparticle (LNP) platform can deliver several of these hits at once. Synthetic mRNA COVID-19 vaccines instruct host cells to produce spike protein from within ionizable LNPs, alongside residual plasmid DNA in some lots. Across the primary literature we identify 35 distinct mechanisms by which the mRNA–LNP platform may induce or accelerate cancer. They converge on four linked routes: (i) protooncogene activation (ii) mutation pressure; (iii) protein–protein interaction (PPI) network interference; and (iv) cancer stem-cell (CSC) clonal acceleration. Where the classical multi-hit clock runs in years, concurrent exposure to oncogenic factors compresses it. The predicted clinical phenotype is therefore not uniform excess incidence but accelerated progression and metastatic outgrowth in susceptible hosts—those carrying dormant micrometastases, clonal hematopoiesis, residual disease after resection, or DNA-repair heterozygosity. Two exposure-stratified population cohorts and one systematic review of the case literature bear on this prediction: (i) A Korean national cohort of 8.4 million subjects reported elevated one-year cancer risk in vaccinated individuals across six sites relative to propensity-matched unvaccinated controls, with platform-specific and dose-dependent patterning. (ii) A 30-month Italian province-wide cohort found higher cancer hospitalization among vaccinated than unvaccinated residents (HR 1.23), attenuating at long lag times — precisely the behavior compressed presentation would produce. (iii) A systematic review of 69 publications documented rapid progression, injection-site and draining-node involvement, and reactivation of controlled disease in 333 patients across 27 countries. The vast majority of these cases occurred following COVID-19 vaccination, with a minority following SARS-CoV-2 infection. Two further signals are ecological rather than individually stratified: (i) Early-onset (age <50 years) cancer incidence in the USA rose approximately 6.4% between 2021 and 2023, from about 109.5 to 116.4 per 100,000, and (ii) Published time-series analysis of CDC WONDER mortality data indicates 154,330 excess US cancer deaths ($z = 15$) after the Week 14, 2021 inflection — the week of peak U.S. mRNA vaccine uptake — with the excess concentrated below age 55 and running roughly twofold higher in the most heavily vaccinated states compared to the least; our own query of the same federal files places the total between approximately 119,000 and 197,000 excess cancer deaths depending on correction for pandemic mortality displacement, bracketing the published estimate. Laboratory, clinical, and population evidence align: the mechanisms predict that mRNA vaccines should accelerate cancer in susceptible people, published patient cases describe exactly that pattern, and national cancer registries record it at scale. Set against a platform whose translational fidelity, nucleic-acid residuals, biodistribution, and long-horizon antigen fate remain uncharacterized, this convergence defines a foreseeable risk that does not require proof of population-level excess incidence before it is acted upon. The first randomized test of this strategy as monotherapy in residual cancer has now failed: a Phase 2 trial of an individualized mRNA neoantigen therapy given as adjuvant monotherapy to 327 patients with molecularly detected residual colorectal cancer crossed its futility boundary and was terminated on a numerical overall survival imbalance. We therefore call for immediate withdrawal of the nucleoside-modified mRNA–LNP platform from broad preventive use and from expanded adjuvant and neoadjuvant oncology, pending independent, lot-linked, multi-omic resolution of persistence, frameshift products, residual DNA, off-target antigen expression, and endpoints of progression and metastasis in high-risk hosts.

Keywords: mRNA vaccine; cancer; spike protein; protooncogene activation; MYC; EGFR; mutation pressure; cancer stem cells; PPI network; frameshifting; residual DNA; neoantigen; multi-hit oncogenesis

1. Introduction: From Sequential Carcinogenesis to Concurrent Pathway Occupancy

Hanahan and Weinberg organized neoplasia around eight hallmark capabilities and enabling traits of genomic instability and tumor-promoting inflammation, later expanded to include phenotypic plasticity [1–3]. Adult solid tumors typically accumulate several driver alterations over decades [4]. The formal basis for that expectation is the multi-hit model of carcinogenesis. Sutherland and Bailar, analyzing colon-cancer incidence, showed that the age-specific incidence curve is well fitted by a process requiring several independent rate-limiting events within a single cell lineage, and set out the etiologic implications of that fit [5]. The model's central consequence is temporal: because the required events are independent and each is individually rare, the waiting time to malignancy is long and incidence rises steeply with age. It follows that any exposure supplying more than one rate-limiting event at the same time, or raising the rate at which such events occur, shortens that waiting time. The concurrent-hit model developed in this review is an application of that logic rather than a departure from it: the arithmetic of the multi-hit model is retained, and only the assumption that the hits arrive separately is relaxed. Inflammation can expand repair-activated stem pools in which mutations are efficiently selected [6–8].

Valdes Angues and Perea Bustos applied the multi-hit framework directly to COVID-19 vaccination, proposing that spike-based products could satisfy its criteria by supplying several rate-limiting events concurrently: induction of lymphopenia and inflammation, downregulation of ACE2 expression, activation of oncogenic cascades, sequestration of tumor-suppressor proteins, dysregulation of the RNA–G-quadruplex protein-binding system, alteration of type I interferon responses, and unsilencing of retrotransposable elements [9]. They attributed these effects to four upstream sources — the pro-inflammatory action of the lipid nanoparticles, the impaired type I interferon response, translational dysregulation of cellular microRNAs by structurally modified mRNA, and the expression pattern, binding profile and tumorigenic properties of the spike protein and its S1 and S2 subunits — and argued that the resulting milieu could both initiate transformation and reawaken dormant cancer cells [9].

Cancer patients were excluded from pivotal randomized trials yet received repeated recommendations for primary series and boosters. The same platform is now advancing into adjuvant oncology. The central clinical question is not only whether the platform can initiate cancer de novo, but whether concurrent hits can accelerate progression and metastatic outgrowth in susceptible hosts—those with dormant micrometastases, clonal hematopoiesis, residual disease after surgery, or DNA-repair heterozygosity [9–12]. In that substratum, the relevant phenotype is compressed time-to-progression, stem-like therapy escape, and dissemination, not solely new primary diagnoses.

The review proceeds in three movements. Sections 2 and 3 establish the exposure: the shared recombinant antigen design encoded as mRNA, the persistence that converts a transient dose into standing pathway input, and the cumulative-dose and residence-time arithmetic that makes concurrent occupancy possible. Sections 4 through 7 develop the four concurrent hits in turn—protooncogene activation, mutation pressure, PPI-network interference, and cancer stem-cell acceleration. Section 8 sets out the platform liabilities that enable them, including residual plasmid DNA and its SV40 elements, RNA:DNA hybrids that shield that DNA from clearance, and translational infidelity, and Section 9 shows how the four act together. Sections 10 through 16 carry the argument into consequence: why concurrent occupancy compresses the cancer clock, why the chassis rather than the payload is the enduring liability and what follows as that chassis is deployed with RSV and influenza antigens alongside spike, the transfer of that chassis into neoantigen cancer therapy together with the off-target antigen-expression hazard specific to it, the authorization

endpoints that were never gated and leave residual DNA unresolved, the population-level cancer signals now reported together with an original analysis of federal mortality files undertaken for this review, the case-level and tissue-level evidence, and the full thirty-five-mechanism inventory. Sections 17 through 20 set out the validation metrics that would confirm or falsify the model, the implications for precision oncology, the existing body of calls for market withdrawal, and the recommendations that follow.

2. Shared Antigen Design: Recombinant Spike Technology Encoded as mRNA

Both mRNA vaccines (BNT162b2, mRNA-1273) and recombinant protein vaccines (e.g., Novavax NVX-CoV2373) use the same core antigen architecture: prefusion-stabilizing K986P/V987P (S-2P) mutations in S2, often furin-site disablement, and codon optimization for high expression [13–20]. The 2P strategy was developed first for recombinant coronavirus spikes to lock the prefusion conformation that maximizes neutralizing epitopes and expression yield; that amino-acid construct was then encoded as mRNA [13,14,17]. Codon optimization raised GC content and codon adaptation index relative to wild-type viral spike, increasing translation potential [16]. **Figure 1** illustrates this identity.

The distinction is delivery, not antigen identity. Recombinant products administer exogenous purified protein; mRNA products instruct host cells to produce the same engineered protein endogenously, inside an inflammatory LNP context, for a duration that has proven longer than original pharmacokinetic models predicted [21–23].

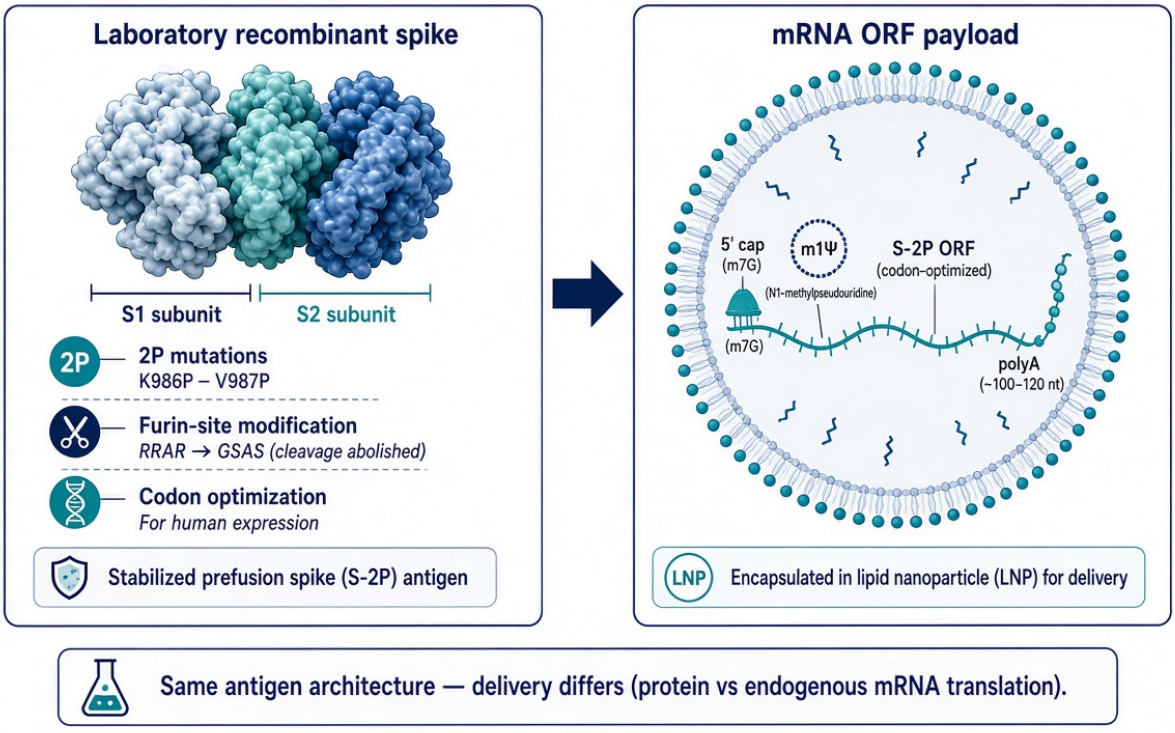

Figure 1. *Shared recombinant S-2P antigen design encoded as mRNA. Laboratory recombinant spike incorporates 2P stabilizing mutations (K986P, V987P), furin-site modification, and codon optimization; the same ORF architecture is delivered as nucleoside-modified mRNA in LNP. Distinction is delivery modality, not antigen identity.*

3. Persistence: How a Transient Dose Becomes Standing Pathway Input

Chronic pathway occupancy requires antigen and nucleic acid that do not clear on the modeled schedule. Circulating spike has been measured after mRNA dosing, including free full-length spike in post-vaccine myocarditis [22,23]. Vaccine mRNA, spike protein, and plasmid backbone fragments have been recovered from blood, exosomes, and tissue more than 3.5 years after the last dose in multi-laboratory case work, with nucleocapsid-negative serology excluding prior infection [21]. Independent series report vaccine-derived S1 within CD16+ monocytes as long as 245 days after dosing in nucleocapsid-negative individuals [24], and mass-spectrometric detection of both full-length and frameshifted recombinant spike proteins in human tissue and circulation after vaccination [25] — the first direct human evidence that the frameshift products predicted by m1Ψ chemistry are recoverable in vivo. Immune cells that take up LNPs release spike- and microRNA-laden exosomes that broadcast signal to distant tissues [11,26]. Residual plasmid DNA, including SV40 promoter/enhancer-ori elements in some Pfizer analyses, adds a second nucleic-acid species co-packaged with LNP delivery [27–30]. Persistence converts a pulse into a standing wave of protooncogene and inflammatory input. Regulatory biodistribution packages that underwrote rapid authorization do not resolve this discrepancy. In Moderna's published rat biodistribution program for mRNA-1273 and related LNPs, of the four lipids in the formulation only the ionizable lipid (lipid H / SM-102 class) was tracked in biodistribution, metabolism, and excretion studies; cholesterol was excluded because endogenous cholesterol cannot be distinguished from product-delivered cholesterol, and DSPC and PEGylated lipids were excluded because they are already present in approved products at higher exposures [31]. That program did quantify two further analytes: vaccine mRNA by RT-qPCR using probes specific to the mRNA-1273 sequence on tissue homogenates, and Spike protein by sandwich ELISA in serum and tissue, from which an effective protein half-life of roughly eighteen hours was derived [31]. The limitations that matter are therefore not the absence of measurement but the boundaries of what was measured, and those boundaries are decisive. Sampling terminated at 336 hours; a fourteen-day observation window cannot speak to persistence at three and a half years, and a negative result inside that window is not evidence of clearance outside it. The Spike ELISA was raised against the intended antigen, but frameshifted polypeptides diverge in amino-acid sequence downstream of the slippery site and would not be captured by an assay built to detect the in-frame product, so the proteomic ensemble actually generated was never enumerated. Residual plasmid DNA was not an analyte at all, and an RT-qPCR assay directed at message does not detect it. Recirculation of released message for multi-pass ribosomal production was not examined, so translation continuing after the tagged-lipid signal declines remains untested rather than excluded. Dosing was supratherapeutic in a rodent model. Notably, the program itself reports occasional detections of mRNA without corresponding lipid H — nucleic acid recovered outside the particle envelope, which is precisely the species a lipid-tracking design is least equipped to follow [31]. Clearance of lipid H and of encapsulated mRNA within days to ~2 weeks in rodent tissues therefore cannot falsify multi-year recovery of vaccine mRNA, spike, and plasmid fragments from human blood, exosomes, and tissue [21]. A study bounded at two weeks, blind to frameshift products and residual DNA, and silent on multi-pass translation cannot be used to declare the platform free of sustained pathway occupancy at multi-year horizons. It was not designed to answer that question, and it does not.

3.1 Cumulative Dose and Temporal Exposure

Persistence and dose are not separate variables. The multi-hit arithmetic is governed by the probability that rate-limiting events coincide within a single lineage, and that probability scales with both the concentration of the insult and the length of time it is present [5,9]. On the pharmacokinetics originally modeled, neither

quantity was expected to be large: a transient pulse of antigen, cleared within days, repeated two or three times across a primary series. The persistence data invalidate that model on both axes simultaneously.

On the temporal axis, vaccine mRNA, spike protein, and plasmid backbone fragments have been recovered from blood, exosomes, and tissue more than 3.5 years after the last dose, in nucleocapsid-negative individuals for whom prior infection is excluded [21]. That is not a long tail on a clearance curve; it is three orders of magnitude beyond the modeled residence time, and it means the exposure interval for any given dose is measured in years rather than days. S1 has been found within CD16+ monocytes at 245 days [24], circulating exosomes carrying spike at four months [26], and frameshifted as well as full-length recombinant spike in human tissue and circulation [25]. Each of these findings represents a separate recovery of product long after it should have been eliminated.

On the dose axis, exposure is cumulative rather than discrete. A primary series plus annual or semi-annual boosters delivers repeated increments of modified mRNA, ionizable lipid, and residual plasmid DNA to a recipient in whom the preceding increments have not been shown to have cleared [21,27–30]. If residence time exceeds the dosing interval — and at 3.5 years it exceeds every dosing interval in use — then successive doses do not replace one another but superimpose. The relevant exposure metric is therefore not dose but the integral of concentration over time, a quantity that no regulatory biodistribution package for these products has ever estimated [31].

Three lines of evidence indicate that the biological response tracks the cumulative rather than the individual dose. IgG4 class switching against spike appears only after repeated dosing and increases with the number of exposures [32]. In a pancreatic adenocarcinoma cohort, IgG4 rose with vaccination number and overall survival fell with repeated boosting [33]. And in solid-tumor patients, cytotoxic T-cell exhaustion markers rose and interferon-γ output fell specifically after the third dose, in patients who had responded optimally to the first two [34]. In each case the effect is absent at low exposure and emerges as exposure accumulates, which is the signature of a cumulative rather than a threshold process.

This has a direct consequence for the concurrent-hit model. The four hits developed in Sections 4 through 7 need not be delivered simultaneously by a single dose. They need only overlap in time. Persistence measured in years against dosing intervals measured in months guarantees that overlap by construction, and each additional dose widens the window in which the hits coincide rather than resetting it. Cumulative dose and residence time are therefore the two variables that convert a set of individually low-probability mechanisms into a plausible concurrent exposure, and both remain uncharacterized in the products' own regulatory files [21,31].

4. Hit One — Protooncogene Activation: EGFR, RAS–MAPK, PI3K–AKT and STAT3–MYC

Protooncogenes are normal cellular genes that promote regulated growth, survival, and differentiation. When chronically activated—by ligand excess, receptor overexpression, activating mutation, amplification, or loss of opposing tumor-suppressor brakes—they become oncogenes and drive the proliferative and survival programs of cancer [1–3]. Protooncogene activation is therefore the conversion of physiologic growth signaling into sustained, ligand- or pathway-driven proliferation that no longer respects tissue checkpoints. In the concurrent-hit model this is the primary proliferative hit (**Figure 2**): persistent occupancy of receptor tyrosine kinase and inflammatory cascades that feed the transcriptional oncogene MYC, while p53/BRCA-dependent brakes are weakened.

Recombinant spike S1/RBD activates EGFR and drives ERK1/2 and AKT phosphorylation at magnitudes comparable to EGF, with induction of the anti-apoptotic protein survivin [35,36]. S1 also triggers ERK in vascular cells independently of ACE2, indicating EGFR-axis input beyond classical viral entry biology [37]. ACE2 downregulation after spike engagement shifts angiotensin signaling toward AT1R, amplifying MAPK, PI3K/AKT/mTOR, NF-κB, AP-1, TGF-β, and IL-6—pathways that reinforce both proliferation and inflammatory stem-cell niches [9,37–40]. Network analyses of SARS-CoV-2 proteins recover SRC, MYC, EGFR, MET, ERBB family members, BRAF, KRAS, JUN, and FOS as recurrent host nodes, placing spike-related signaling squarely inside the classical protooncogene map [39,41].

MYC is the transcriptional integrator of this hit. It amplifies expression of genes required for cell-cycle progression, metabolism, and biomass accumulation; dosage variation—including via extrachromosomal DNA—drives phenotypic plasticity and niche independence [42]. Bulk RNA-seq from patients with new-onset post-vaccination cancer shows enrichment of MYC-target programs and suppression of tumor-control signatures, consistent with pathway-level activation rather than isolated receptor noise [12]. IL-6–STAT3 signaling, fed by LNP and spike-associated inflammation, further induces MYC and anti-apoptotic proteins, coupling innate inflammatory stress to the protooncogene [3,43].

Suppressor failure is the complementary face of the same hit. Tumor suppressors such as p53 and BRCA1/2 normally restrain protooncogene output by enforcing DNA-damage checkpoints, apoptosis, and homologous recombination. Spike expression interrupts p53–MDM2 dynamics, suppresses p53 activation of p21(WAF1), DR5, and MDM2, and increases viability after chemotherapy in experimental systems [44]. S2 has been implicated in interactions with p53 and BRCA1/2 [9,37,44]. When growth pathways are occupied and suppressor brakes are compromised, a physiologic growth signal becomes an oncogenic program: sustained proliferation, apoptosis resistance, and a cellular state primed for the mutation-pressure and stem-cell hits that follow.

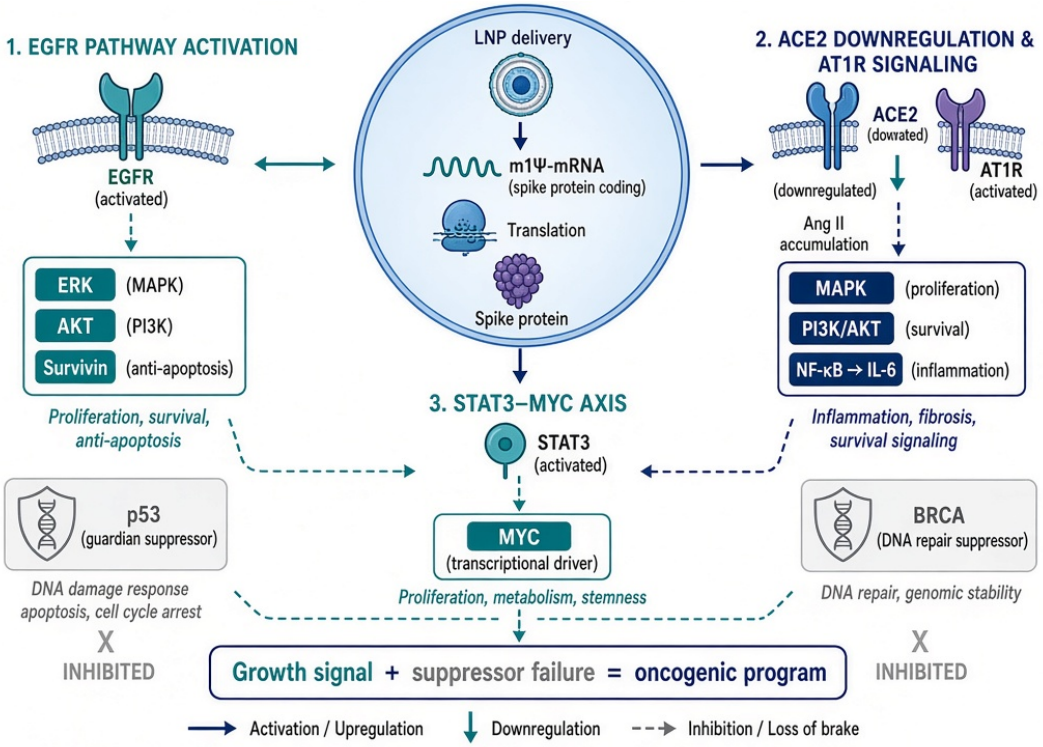

Figure 2. *Protooncogene activation. LNP-delivered m1Ψ-mRNA is translated to spike, which occupies EGFR (ERK/AKT/survivin), drives ACE2 downregulation toward AT1R (MAPK/PI3K/NF-κB/IL-6), and feeds the STAT3–MYC axis while p53 and BRCA suppressor brakes are inhibited—converting a growth signal into an oncogenic program.*

5. Hit Two — Mutation Pressure: Repair Failure, LINE-1 Unsilencing and Genomic Integration

Multi-hit arithmetic requires either a higher mutation rate or an expanded at-risk stem-cell pool in which drivers are efficiently selected [4,7]. The nucleoside-modified mRNA–LNP platform can raise mutation pressure through five cooperating processes (**Figure 3**). First, DNA-repair interruption: spike-associated disruption of p53–MDM2 dynamics and reduced p53 transcriptional output (p21, DR5, MDM2) weaken G1/S and apoptotic checkpoints, while reported interference with BRCA1/homologous recombination and NHEJ leaves double-strand breaks unresolved and favors error-prone end joining [9,37,44]. Cells that continue cycling with unrepaired lesions accumulate insertions, deletions, and chromosomal rearrangements—the genomic instability hallmark of multi-hit carcinogenesis. Second, LINE-1 unsilencing: inflammatory and interferon-perturbed states can derepress long interspersed element-1 retrotransposons; in vitro, vaccine RNA has been reverse-transcribed in LINE-1–competent cells, creating a theoretical substrate for chimeric cDNA [45,46]. Third, rare but high-impact host–vector chimeric events: a documented chimeric read in circulating tumor DNA from rapidly progressive stage-IV bladder cancer mapped to a non–safe-harbor locus on 19q13.42, illustrating that even infrequent integration-class events can land in gene-rich oncogenic neighborhoods [10]. Lipid-based transfection establishes a non-trivial baseline probability for this class of event: end-modified linear DNAs integrate spontaneously in roughly 1–10% of transfected mammalian cells [47]. Fourth, ribosomal and nonsense-mediated-decay (NMD) stress: G-quadruplex-rich, m1Ψ-modified messages promote +1 frameshifting and stalled ribosomes; the resulting out-of-frame polypeptides and NMD load drive proteostatic stress and can elicit error-prone compensatory transcription, expanding mutational opportunity without requiring classical mutagens

[11,12,48]. Fifth, LNP-driven inflammatory reactive oxygen species and epigenetic imprinting of stem cells that persist after the acute insult resolves, locking an expanded, repair-activated stem pool into a higher-risk state for subsequent driver capture [6,49]. Sixth, the residual DNA is not sequence-neutral. The production plasmids carry SV40 regulatory elements whose documented activities bear directly on mutation pressure: the SV40 enhancer functions as a somatic hypermutation-targeting element that recruits APOBEC3/AID cytidine deaminases and drives C-to-T transitions, an established route to lymphomagenesis [50]; the enhancer also contains a nuclear targeting sequence that facilitates import of otherwise cytoplasmic DNA into the nucleus [51]; SV40-based constructs demonstrate integration capability with durable transgene expression [52]; and the ColE1/pMB1 bacterial origin, which sits adjacent to the spike sequence, is a known cryptic mammalian promoter [53]. p53 additionally represses SV40 early transcription through the promoter region [54], raising an untested question of whether promoter-bearing fragments could titrate suppressor protein in trans. A fragment bearing these elements is therefore not inert filler but a sequence with nuclear-import, mutagenic, promoter, and integration functions annotated in the literature. Together these processes do not each need to generate a full complement of drivers; they raise the probability that the next driver occurs inside a self-renewing, immune-evasive cell—the operational definition of mutation pressure under concurrent hits.

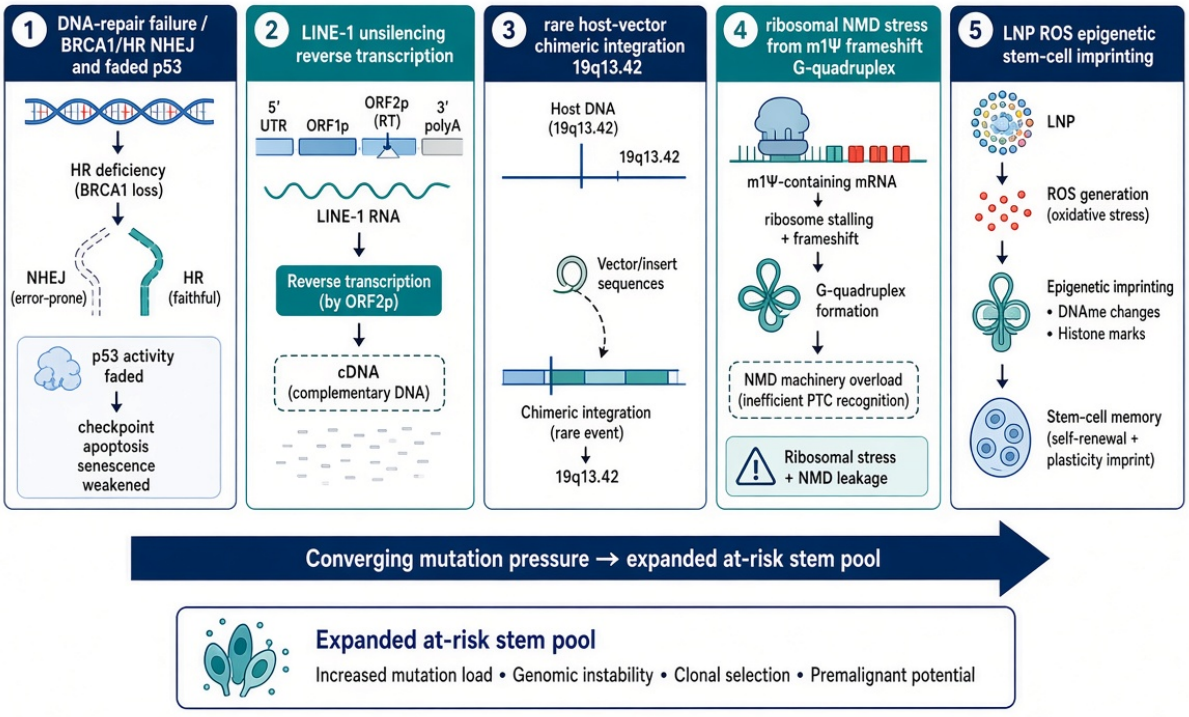

Figure 3. *Mutation pressure—five cooperating sources: (1) DNA-repair failure (BRCA1/HR, NHEJ) with faded p53; (2) LINE-1 unsilencing and reverse transcription; (3) rare host–vector chimeric integration (e.g., 19q13.42); (4) ribosomal/NMD stress from m1Ψ frameshift and G-quadruplex structure; (5) LNP ROS and epigenetic stem-cell imprinting. Convergence expands the at-risk stem pool.*

6. Hit Three — Protein–Protein Interaction Network Interference

Protein–protein interaction (PPI) networks are the operational wiring of the cell. Receptors, kinases, scaffolds, suppressors, and transcription factors function as dynamic complexes whose composition and post-translational state determine signal flow. Oncogenesis is, in large part, a problem of rewired PPIs: new

edges appear, physiologic edges are lost, and information is redirected toward proliferation, survival, invasion, and stemness [55,56]. In the concurrent-hit model, PPI interference is the process that converts local ligand occupancy into multi-hallmark occupancy—and, in susceptible hosts, into network states that favor accelerated progression and metastatic competence.

6.1 How the platform rewires network edges

Interference is not limited to one protein binding another. It includes direct physical contact (spike or frameshift product binding to a host protein); receptor occupancy and dimerization bias (EGFR, ACE2–AT1R, CD147); post-translational state change (phosphorylation or ubiquitination that switches affinity); expression-level rewiring (transcriptional change in interaction partners); scaffold or localization shift (membrane ↔ cytosol ↔ nucleus); and indirect cascades driven by cytokines, ROS, or exosomal microRNAs that alter partner availability without direct viral contact. Any of these can percolate across modules.

6.2 The four controlling hubs: EGFR, MYC, p53 and STAT3

Cancer PPI networks are not uniform. A small number of hubs carry disproportionate betweenness. EGFR sits at the boundary of receptor tyrosine kinase, RAS–MAPK, and PI3K–AKT modules; spike S1/RBD can activate EGFR and drive ERK/AKT phosphorylation at magnitudes comparable to EGF [35,36], positioning persistent spike-like input to rewire downstream complexes. Oncogenic KRAS extensively rewires the EGFR interactome—thousands of mapped PPIs change through expression, phosphorylation, and binding dynamics, redirecting flow toward MYC and related transcription factors [56]. MYC is both a client of upstream RTK/STAT input and a rewiring agent of its own interactome; MYC-target enrichment in post-vaccination cancer transcriptomes implies shifted MYC-containing complexes as well as higher activity [12,42]. p53 is the suppressor hub: spike-associated interruption of p53–MDM2 dynamics and reduced p53 transcriptional output remove braking edges to repair and apoptosis while proliferative edges remain intact [44]. STAT3 bridges inflammatory input to MYC, survival genes, and, in some contexts, EGFR itself via a pSTAT3–EGFR feedback loop [3], linking innate-sensing to kinase–transcription and stemness clusters.

6.3 How damage spreads between clusters

The modules in **Table 1** are not isolated. Pathologic edge gain propagates from the receptor cluster (EGFR, ACE2/AT1R, CD147) into the kinase–transcription cluster (RAS–ERK, PI3K–AKT, NF-κB, STAT3–MYC), while physiologic edges in the tumor-suppressor cluster (p53–MDM2, BRCA1/2) and innate-sensing cluster (type I IFN) are weakened. Stemness-module edges (Wnt, Notch, Hedgehog, Sox2/Oct4) are strengthened. The resulting network state favors proliferation, survival, immune evasion, and invasive stem-like identity simultaneously—the network basis of multi-hallmark occupancy and of dissemination-competent clones.

6.4 Platform-specific sources of network interference

In-frame spike contributes ligand-like engagement of EGFR and ACE2-axis partners, ER/Golgi trafficking stress, and surface/shed autocrine edges. Frameshifted polypeptides (m1Ψ-dependent) introduce sequence-divergent proteins with unpredictable binding surfaces and potential dominant-negative or neo-interactions [48]. Residual plasmid DNA acts indirectly through DNA-sensing pathways that change phosphorylation

state of network hubs. LNP inflammation (IL-1β, IL-6, ROS) and exosomal microRNA/spike cargo export perturbation to distant cells [11,26]. Persistence is decisive: transient PPI changes can resolve; sustained antigen keeps the rewired state from relaxing and turns a pulse into a new steady-state interactome capable of supporting prolonged clonal selection.

6.5 Link to metastatic competence

PPI interference is the wiring diagram through which the other hits become concurrent. Protooncogene activation is physically realized as strengthened edges from EGFR/STAT3 into RAS–MAPK, PI3K–AKT, and MYC complexes. Mutation pressure is amplified when p53/BRCA edges to repair machinery are lost. CSC acceleration and metastatic competence follow when edges into Wnt/Notch/Hedgehog are gained and IFN-surveillance edges are lost, selecting stem-like cells with invasive and immune-evasive properties. In susceptible hosts—residual disease, clonal hematopoiesis, DNA-repair heterozygosity—this rewired graph is the network substrate of accelerated progression and metastatic outgrowth.

6.6 How network interference can be measured

PPI interference is measurable by affinity purification–MS or BioID of EGFR, MYC, p53, and STAT3; phosphoproteome distance metrics; proximity ligation for key pairs (EGFR–GRB2, p53–MDM2, STAT3–MYC); and network statistics (hub betweenness, modularity between receptor and stemness clusters, information-flow models as applied to KRAS-rewired EGFR networks [56]). A research-positive call requires significant pathologic edge gain and suppressor/IFN edge loss at ≥2 hubs, co-occurring with platform persistence markers and at least one other concurrent-hit domain.

Cluster	Nodes	Consequence	Refs
Receptor	EGFR, ACE2/AT1R, CD147, ER	Ligand-like protooncogene input	[35,40,41]
Kinase–transcription	RAS–ERK, PI3K–AKT–mTOR, NF-κB, STAT3–MYC	Proliferative and survival transcription	[35,39,56]
Tumor-suppressor	p53–MDM2, BRCA1/2, ATM/MSH2	Repair and apoptosis failure	[44,55]
Innate sensing	TLR–IRF, RIG-I, type I IFN, cGAS–STING	IFN interruption + chronic innate noise	[11,49]
Stemness	Wnt, Notch, Hedgehog, Sox2/Oct4	CSC conversion and niche independence	[8,57,58]

Table 1. *Cross-cluster PPI modules engaged by persistent spike, LNP, and exosomal cargo.*

7. Hit Four — Cancer Stem-Cell Acceleration and Dormancy Escape

CSCs are units of initiation, therapy escape, metastatic dissemination, and rapid relapse [8,57]. They are expanded by inflammation, protooncogene dosage, and suppressor loss [7,43,49,57]. Four cooperating inputs accelerate the clone (**Figure 4**): (1) EGFR/PI3K/STAT3/MYC stabilization of Wnt/Notch/Hedgehog stem states that confer invasive and niche-independent behavior [8,57]; (2) inflammatory epigenetic imprinting of stem cells that persists after resolution [6]; (3) type I IFN blunting from m1Ψ chemistry plus lymphopenia, favoring immune-evasive CSC selection and reduced metastatic immunosurveillance [9,11]; (4) mutation pressure inside an expanded stem pool so the next driver occurs in a self-renewing, dissemination-competent cell [4,10,49]. When these inputs arrive together, the classic multi-hit clock (years) compresses toward months: residual or occult clones can expand, evade, and seed distant sites faster

than sequential models predict. The clinical correlate is accelerated progression and metastatic risk in susceptible hosts, not uniform excess incidence in every recipient. Independent lines of evidence now support the dormancy-awakening step specifically, and by more than one route. Respiratory viral infection reawakens dormant metastatic breast cancer cells in the lung through interferon-driven STAT1–NF-κB remodeling of the metastatic niche [59]; the ionizable lipid nanoparticles used in these vaccines, administered without any mRNA cargo, drive neutrophil recruitment and neutrophil extracellular-trap formation in lung, an established mechanism for awakening dormant cancer cells, and thereby promote metastatic outgrowth in mice [60]; patients with glioblastoma showed accelerated tumor progression after SARS-CoV-2 infection in a retrospective case–control analysis [61]; and repeated COVID-19 booster vaccination was associated with worse overall survival and elevated IgG4 in a 96-patient pancreatic adenocarcinoma cohort [33]. The first of these is mechanistically instructive in a direction that cuts against a simple interferon-blunting account: there, type I/II interferon signaling was the awakening stimulus rather than its absence, indicating that both excess and deficit of interferon tone may destabilize dormancy depending on timing and compartment [59].

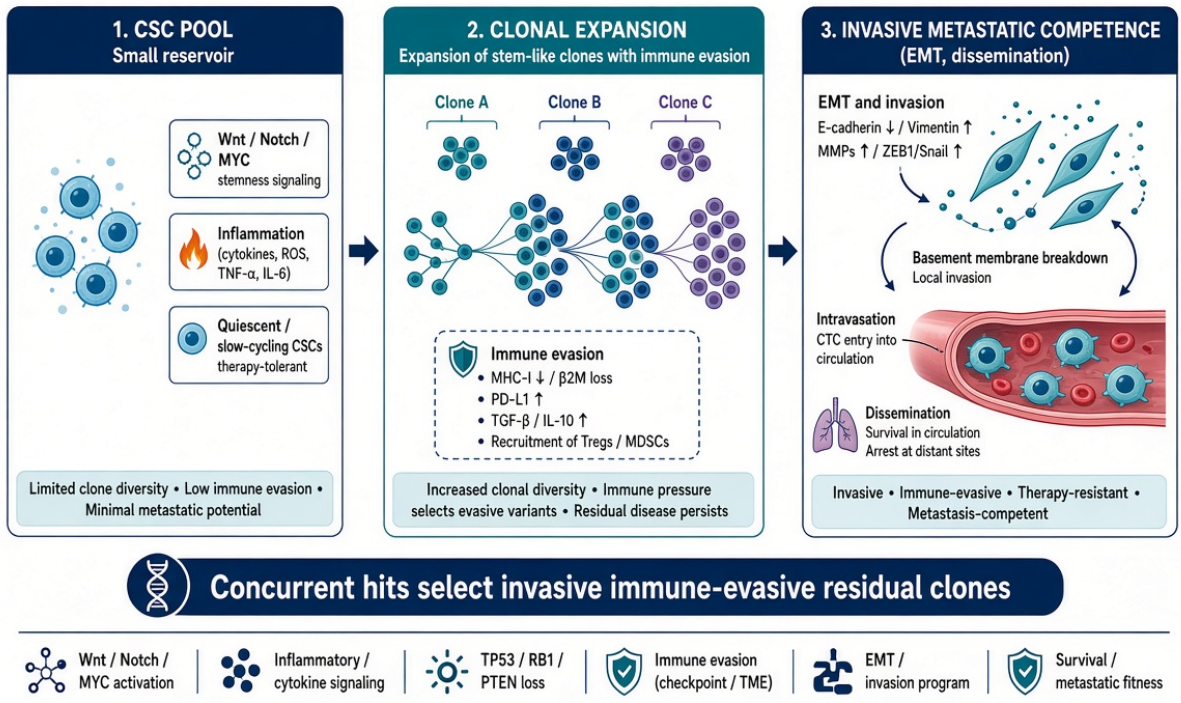

Figure 4. *CSC clonal acceleration and metastatic competence. A minority CSC pool under Wnt/Notch/MYC and inflammation expands into immune-evasive clones with EMT, intravasation, and disseminated metastatic potential—selection of invasive residual disease under concurrent hits.*

8. Platform Liabilities: Residual DNA, Frameshifting and Translational Infidelity

With the four concurrent hits defined, the enabling platform defects come into focus. The platform was authorized under emergency frameworks that prioritized short-term immunogenicity. Multi-year persistence, finished-product residual-DNA fragment-length distribution, frameshift proteomics, and cancer-registry linkage with dose/lot resolution were not gate criteria [9,27–30,62]. Cancer patients—the population most sensitive to protooncogene activation and stem-cell selection—were largely excluded from pivotal trials.

N1-methylpseudouridine was introduced to reduce innate sensing and raise protein yield [63,64]. Mulroney et al. demonstrated that m1Ψ causes +1 ribosomal frameshifting at slippery sequences, generating out-of-frame polypeptides; cellular immunity to those products was detected in vaccinated humans [48,65]. Sequence optimization can reduce slippery sites [66]; that optimization was not a precondition of first-generation products.

Independent laboratories have reported residual plasmid DNA, including SV40 promoter/enhancer-ori sequences in some Pfizer lots, with ongoing dispute over fluorometric versus qPCR methods, drug-substance versus drug-product testing, and regulatory significance [27–30]. Regulators maintain that fragments are non-infectious, below concern thresholds in validated assays, and not shown to cause genotoxicity at population scale [62], and a recent four-platform analysis reporting no excessive impurities has been cited in support of that position [67]. The dispute is now specific rather than general. A published methodological critique identifies six biases in that analysis, all running in the direction of underestimation: conversion of qPCR copy number to mass using intact plasmid molecular weight without fragmentation correction; amplicon-size bias that systematically underdetects the spike target relative to shorter backbone amplicons; heat-induced degradation during library preparation; a capillary-electrophoresis detection floor above the regulatory threshold itself; short-read platform exclusion of kilobase-length fragments that long-read sequencing recovers; and failure to account for RNA:DNA hybrids [68]. On the critique's arithmetic, applying the fragmentation correction to the smallest amplicon alone moves the reported value above the 10 ng regulatory limit [68]. The structural liability is that LNP-delivered DNA is not equivalent to free DNA in older biologics, and finished-product transparency lagged deployment.

The RNA:DNA hybrid mechanism deserves separate statement because it explains why residual DNA persists at all. DNase I, the standard step for removing the DNA template after in vitro transcription, has a specific activity against RNA:DNA hybrids at least 100-fold below that against double-stranded DNA [69]. This is not a contested claim: BioNTech investigators state it directly, noting that residual RNA:DNA hybrids may therefore be co-isolated with the single-stranded mRNA product [70]. Independent work reports that spike-encoding sequences are enriched in hybrid form and that lipid nanoparticle encapsulation shields them from cellular nucleases, and offers this as the explanation for the 4–6 cycle-threshold gap consistently observed between spike and backbone amplicons of comparable length [68,71]. The nuclease deficit itself is not in dispute; what remains preprint-stage is only the magnitude of spike enrichment. Either way the implication runs against the reassurance: the sequence of greatest biological concern is the one most protected from the clearance step, and quantification methods calibrated on naked DNA will systematically miss it.

The manufacturers have described the resulting hazard in their own patent filings, in terms the present review need not improve upon. Moderna states that residual DNA in drug products "may induce activation of the innate response and has the potential to be oncogenic in patient populations" [72]. The same filings note that introduced DNA "can integrate into host cell genomic DNA at some frequency, resulting in alterations and/or damage to the host cell genomic DNA," and that such heterologous DNA "can be inherited by daughter cells (whether or not the heterologous DNA has integrated into the chromosome) or by offspring" [73]. Integration frequency, oncogenic potential, and heritability are therefore not adversarial characterizations of the platform. They are the developer's own stated understanding of what residual DNA can do, recorded before deployment and not subsequently resolved by measurement in finished product.

The intended proteomic output was a single clean prefusion trimer, briefly expressed. The actual ensemble can include in-frame spike, frameshifted polypeptides, residual nucleic acids, prolonged circulating antigen, and proteostatic stress (**Figure 5**) [12,21,22,48].

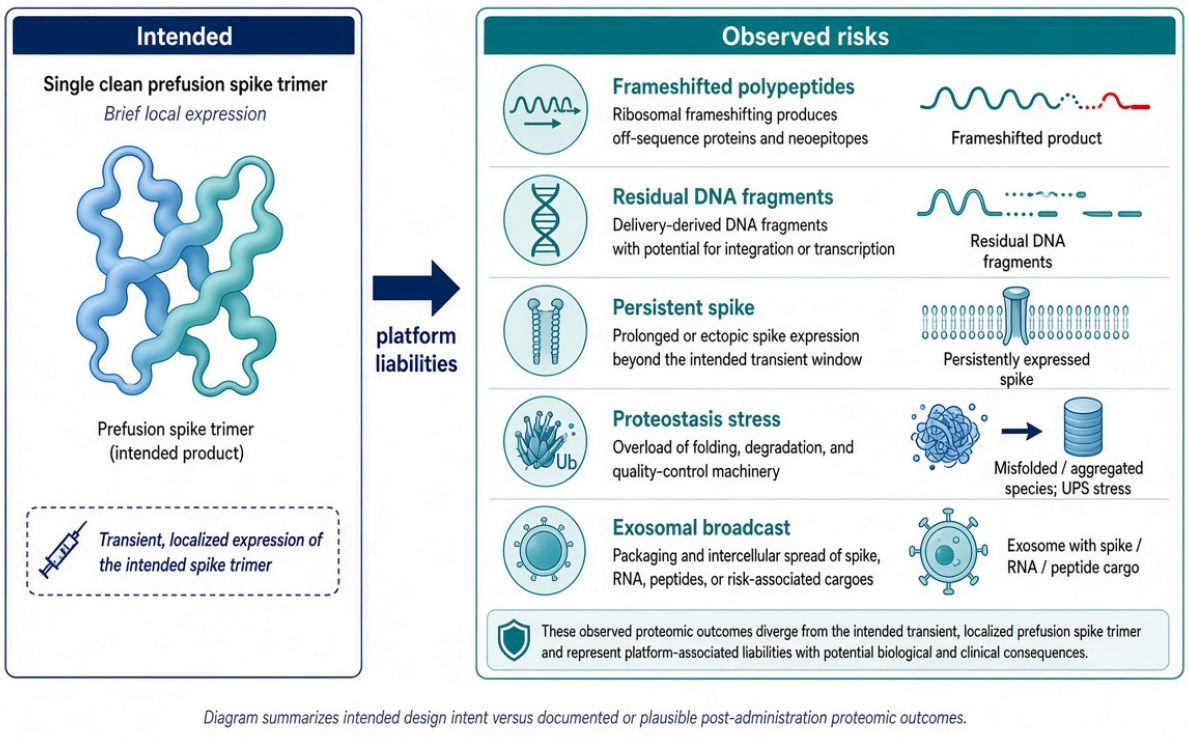

Figure 5. *Intended versus actual proteomic ensemble. Intended: single clean prefusion spike trimer with brief local expression. Observed platform risks: frameshifted polypeptides, residual DNA fragments, persistent spike, proteostasis stress, and exosomal broadcast.*

9. Synthesis: How the Four Hits Act Together

The four hits developed above are not independent processes running in parallel; they are coupled outputs of a single sustained exposure, and each lowers the threshold for the others. Their mechanisms and the cancer hallmarks each engages are summarized in (**Table 2**).

Hit	Mechanism	Hallmark engaged	Refs
1. Protooncogene activation	EGFR–RAS–MAPK, PI3K–AKT, STAT3–MYC	Proliferation, survival, plasticity	[35,36,39]
2. Mutation pressure	Repair failure, LINE-1, NMD stress, rare integration	Genomic instability	[39,45–47]
3. PPI cross-cluster interference	Rewiring at EGFR, MYC, p53, STAT3 hubs	Multi-hallmark occupancy	[41,55,56]
4. CSC clonal acceleration	Wnt/Notch/MYC, inflammatory imprint, IFN evasion	Initiation, relapse, compressed kinetics	[6,8,57,59]

Table 2. *Concurrent-hit model.*

Infection can occupy some of the same nodes [37–41]. The vaccine-specific increment is systemic LNP inflammation, modified RNA with prolonged half-life, codon/G-quadruplex architecture, residual DNA,

repeated dosing without mucosal constraint, and documented multi-year persistence [11,21,48,49]. In susceptible hosts these increments are predicted to favor accelerated clonal dominance and metastatic competence rather than only de novo initiation. Context matters: selected immunotherapy-context series report possible benefit from peri-operative mRNA vaccination; those observations do not cancel protooncogene activation or CSC-driven progression risk in treatment-naïve or immunocompromised hosts [74].

10. Why Concurrent Hits Compress the Cancer Clock

Sections 2 through 9 established the exposure, the four hits, and the platform liabilities that enable them. What remains is to say why that combination matters clinically, and the answer turns on timing. The classical multi-hit model assumes temporal separation: successive drivers accumulate over years within a constrained stem pool. The concurrent-hit framing asks what happens when several hallmarks are occupied at once by a single exposure class. Protooncogene activation, mutation pressure, PPI rewiring, and CSC acceleration are linked consequences of persistent engineered antigen, inflammatory LNP chemistry, imperfect translational fidelity, and residual nucleic acids. When those inputs coincide, the calendar separating residual disease from clinically overt progression or metastasis can compress. Susceptibility concentrates where dormant clones, clonal hematopoiesis, DNA-repair heterozygosity, or residual microscopic disease already exist—the hosts in whom accelerated progression and metastatic outgrowth are the primary clinical concern.

11. The Payload Changes, the Chassis Does Not

Early literature focused on spike as ligand for EGFR, ACE2–AT1R, and related pathways—valid, because vaccine spike is the recombinant S-2P architecture delivered endogenously. Persistence converts a transient immunogen into standing pathway input. Structural liabilities, however, are not spike-specific: m1Ψ-dependent frameshifting, residual plasmid DNA, ionizable-lipid inflammation, systemic biodistribution, and incomplete multi-year proteomic characterization are properties of the nucleoside-modified mRNA–LNP platform. Any ORF—viral glycoprotein or tumor neoantigen cassette—rides the same chassis.

That the vehicle itself carries oncologic liability is no longer inference. In a 2026 study using ALC-0315 and ALC-0159 — the ionizable and PEGylated lipids of the Comirnaty formulation — intramuscular administration of lipid nanoparticles containing no mRNA at all promoted lung metastasis in mice [60]. The effect was dose-dependent, reproduced in both B16-F10 melanoma and 4T1 breast carcinoma models, and occurred whether the particles were given before tumor inoculation or seventy-two hours after it. The mechanism is specified: intramuscular injection caused necrosis of muscle cells at the injection site, releasing mitochondrial DNA; that mtDNA activated TLR9–MyD88 and cGAS–STING signaling; the resulting neutrophil recruitment to lung produced neutrophil extracellular traps; and those traps established a pre-metastatic niche, with histone H3 mediating adhesion of tumor cells to endothelium. Inhibiting NET formation with DNase I reduced the metastatic burden [60].

Three features of that result bear directly on the present argument. It is payload-independent by construction — there was no encoded antigen, so nothing in the finding depends on spike, on a neoantigen cassette, or on any open reading frame. It supplies a mechanistic bridge between two liabilities catalogued separately in this review, ionizable-lipid inflammation and cytosolic DNA sensing, and terminates them in a metastatic rather than a merely inflammatory endpoint. And it reaches dormancy escape by a second route: neutrophil extracellular traps are an established mechanism for awakening dormant cancer cells [60], which is the

phenotype Section 7 develops through interferon-driven niche remodeling. The authors note that murine and human immune architecture differ and that their findings may not fully recapitulate clinical use. The finding nonetheless establishes in vivo that the delivery vehicle, absent any cargo, is sufficient to accelerate metastatic outgrowth in a host carrying tumor cells — which is the host context this review identifies as decisive.

11.1 An Expanding Array of Persistently Expressed Antigens

That argument is no longer hypothetical, because spike is no longer the only antigen this chassis delivers. mRESVIA (mRNA-1345) encodes the stabilized prefusion F glycoprotein of respiratory syncytial virus and is approved in more than forty countries, initially for adults aged 60 and over and subsequently for at-risk adults aged 18 to 59; it uses the same lipid nanoparticle system as the COVID-19 products [75]. mFLUSIVA (mRNA-1010) encodes influenza hemagglutinins and was approved by the FDA in August 2026 for adults aged 50 and over, the first mRNA influenza vaccine licensed in the United States [76]. A combined influenza–COVID product, mRNA-1083, is under regulatory review. The chassis is therefore being deployed with at least three distinct antigen classes into overlapping populations on recurring seasonal schedules.

Each of these products instructs host cells to synthesize a foreign glycoprotein endogenously, within an inflammatory lipid context, for a duration that has not been established for any of them. The persistence work that documented vaccine mRNA, spike, and plasmid fragments beyond 3.5 years was performed on COVID-19 products [21]; no equivalent long-horizon characterization has been published for RSV prefusion F or for influenza hemagglutinin delivered by the same route. The relevant question is not whether these antigens share spike's specific receptor interactions — they do not — but whether the platform-level liabilities established in Section 8 travel with them. Frameshifting is a property of m1Ψ chemistry and slippery-sequence architecture, not of the spike sequence [48,63,64]. Residual plasmid DNA and its regulatory elements are a property of the manufacturing route [27–30]. Ionizable-lipid inflammation is a property of the delivery vehicle [49]. None of these is payload-dependent.

The immunological consequence is additive in a way that single-product analysis does not capture. Each persistent foreign antigen occupies a share of the cytotoxic T-cell and innate surveillance capacity that would otherwise be available for the recognition of transformed cells. The mechanisms developed in Sections 4 through 7 — type I interferon modulation, IgG4 class switching under repeated exposure, lymphopenia, and antigen-driven cytotoxic T-cell exhaustion — are responses to sustained antigen presence rather than to any particular epitope [9,11,32,34]. A recipient receiving a seasonal COVID-19 booster, an RSV vaccine, and an annual mRNA influenza vaccine is not receiving three independent exposures to be assessed separately. They are three concurrent, long-residence antigen loads delivered by the same inflammatory vehicle into the same immune compartment.

Whether the combined effect is additive or synergistic is unknown, and we do not assert that it is synergistic. We note that the question has not been asked. Coadministration data were limited at the time of the influenza approval, and the endpoints assessed were immunogenicity and short-term reactogenicity rather than cumulative antigen burden, surveillance capacity, or time-to-malignancy in susceptible hosts [76]. The concurrent-hit model predicts that risk scales with the integral of antigen exposure over time, not with the number of products; on that prediction, a recipient of three persistent mRNA antigens is a higher-exposure host than a recipient of one, and should be studied as such. No surveillance system presently distinguishes them.

12. Transfer of the Same Platform into Cancer Therapy

Moderna's individualized neoantigen program (mRNA-4157 / intismeran autogene / V940), with Merck, encodes up to 34 patient-specific neoantigens in modified mRNA formulated in proprietary LNPs and is in Phase 3 for adjuvant melanoma, NSCLC, and related settings, typically with pembrolizumab [77–80]. Additional assets encode shared cancer-testis antigens, tumor-associated antigens, frameshift peptides (including Lynch-syndrome prevention concepts), and checkpoint-related targets [81]. BioNTech and others maintain parallel programs. Industry disclosures credit COVID-era platform validation—scale, LNP formulation, rapid construct swapping—as enabling oncology expansion [77,79].

Personalized neoantigen selection is a genuine design advance over a universal viral antigen. It does not erase platform-level risks. Cancer patients receiving adjuvant mRNA therapy already harbor residual disease risk, genomic instability, and stem-like clones—the precise context in which concurrent protooncogene activation, mutation pressure, and CSC selection are predicted to accelerate progression and metastatic outgrowth. Checkpoint combination can amplify desired T-cell responses while intensifying inflammatory stress. Shared-antigen cassettes reintroduce off-tumor concerns that LNP intensity and documented multi-year persistence magnify rather than merely risk magnifying. Spike was the first industrial payload; the oncology pipeline applies the same modality to the most vulnerable hosts under a claim that pandemic-scale use validated the technology. Short-term immunogenicity is not long-horizon safety validation against accelerated progression or metastatic risk in residual-cancer populations.

12.1 Neoantigen mRNA Architecture: No Spike, Same Chassis

Personalized neoantigen mRNA therapy—exemplified by Moderna's intismeran autogene (mRNA-4157 / V940), developed with Merck—does not encode SARS-CoV-2 spike. The open reading frame is a patient-specific concatemer of up to 34 tumor-derived neoepitopes selected by next-generation sequencing of tumor and matched normal tissue, HLA typing, and a proprietary immunogenicity-ranking algorithm [77–79]. A single mRNA molecule carries the concatenated neoantigen cassette (typically on the order of ~75 nucleotides per epitope within the ORF), with engineered 5′ cap, optimized untranslated regions, and poly(A) tail; uridines are replaced by N1-methylpseudouridine (m1Ψ). The construct is formulated in proprietary ionizable lipid nanoparticles (SM-102–class chemistry shared with Moderna's COVID platform lineage) and administered intramuscularly, with manufacturing designed as one lot per patient and a turnaround on the order of weeks from sequencing to product [79,82].

Thus the relationship to spike is platform continuity, not antigen identity. COVID mRNA vaccines encoded recombinant prefusion-stabilized spike (S-2P) as the sole immunogen. Neoantigen INT encodes tumor mutations only. What is shared is the nucleotide and delivery architecture: nucleoside-modified IVT mRNA, LNP encapsulation, plasmid-templated manufacturing with residual-DNA risk, m1Ψ-dependent translational behavior including documented +1 frameshifting risk at slippery sequences, systemic inflammatory LNP chemistry, and incompletely characterized multi-year persistence of product species [12,27,48,79,82]. Industry disclosures explicitly treat pandemic-scale COVID deployment as validation of this chassis for oncology.

It is essential to place this architecture against the background of global exposure that has already occurred. Billions of people received one or more doses of spike-encoding mRNA–LNP products; a large fraction of residual-cancer and adjuvant candidates therefore already carry the molecular footprint of prior spike-driven pathway occupancy—EGFR–MAPK/AKT input, inflammatory LNP pulses, possible frameshift

products, residual nucleic acids, and, in documented cases, multi-month to multi-year product persistence [3,10,12,21,35–37,40–42,44,48,49]. That prior exposure is not erased when the ORF is switched to neoantigens. It is an inherited concurrent-hit base: protooncogene-pathway priming, mutation-pressure and stem-cell stress from the COVID campaign, followed by serial re-challenge of the same chassis in a host who already harbors residual disease. In the concurrent-hit model, the first mass payload (spike) and the second (neoantigen cassette on the identical vehicle) are sequential insults to the same risk-bearing architecture.

Intismeran autogene (mRNA-4157 / V940) works by sequencing a resected tumor, ranking private neoepitopes, and encoding up to 34 of them as a single patient-specific m1Ψ-mRNA concatemer in an SM-102–class LNP; the product is given intramuscularly in serial doses (up to nine, often on a multi-week schedule) together with PD-1 blockade, so that host cells translate the neoantigen cassette and present it to T cells [77–79,82,83]. That mechanism is immunologically rational as adjuvant therapy after complete resection. It is also a mega-dose, multi-cycle re-exposure of residual-disease hosts to the same nucleoside-modified mRNA–LNP chassis that already carried spike to the global population—exactly the setting in which concurrent-hit acceleration of residual clones is most consequential. Independent clinical commentary has framed the current commercial push as an "mRNA gold rush": rapid regulatory trajectories, press-release topline Phase 3 claims without fully public hazard ratios and confidence intervals at announcement, high projected costs, risk of tumor immune escape under serial antigenic pressure, and accumulating long-term platform safety questions that were not closed for COVID products and are not closed for oncology transfer [84]. None of those concerns is answered by renaming the product a "therapy" rather than a vaccine; the chassis—m1Ψ chemistry, inflammatory LNP, residual DNA risk, frameshift potential, and incompletely characterized multi-year persistence—remains.

For the concurrent-hit model this distinction remains decisive—unless neoantigen selection is cross-reactive to similar PPI aberrancy already established by prior spike-pathway occupancy. Protooncogene activation and PPI occupancy driven by spike protein itself are not expected from a pure neoantigen cassette whose epitopes are private tumor mutations. If, however, selected neoepitopes (or frameshifted by-products of the cassette) engage the same hubs—EGFR, MYC, p53/BRCA edges, STAT3—or stabilize the same cross-cluster edges already primed by prior spike-mRNA exposure, the antigen distinction collapses and the two payloads become functionally convergent at the network level. Independent of that contingency, platform-level hits—frameshifted polypeptide ensembles, residual nucleic acids, chronic innate and ribosomal stress, inflammatory stem-cell selection, and any prolonged expression of encoded peptides in a residual-disease host—remain fully applicable and are additive to whatever spike-related occupancy already exists from prior vaccination. Patients receiving adjuvant INT already have residual microscopic disease, genomic instability, and stem-like clones; they are the population in which concurrent CSC acceleration and metastatic competence matter most, and many of them are not vaccine-naïve. Serial LNP dosing (up to nine administrations) re-challenges that high-risk substrate with the same imperfect vehicle whose biodistribution package never tracked free mRNA, frameshift products, or multi-year nucleic-acid persistence [31]. A better payload (true neoantigens matched to HLA) does not erase an imperfect vehicle, does not reverse prior platform exposure, and does not guarantee absence of network cross-reactivity with pathways already stressed by spike. Extension of the same unforeseen liabilities into residual-disease oncology therefore does not soften the case for withdrawal—it makes withdrawal the only proportionate action pending independent multi-omic resolution of fidelity, residuals, persistence, PPI cross-reactivity, and progression endpoints [31,85–88].

Spike was the first mass payload on this chassis; personalized neoantigen mRNA uses the same nucleotide-modified LNP architecture without encoding spike—so residual-cancer hosts inherit platform liabilities (fidelity, residuals, inflammation, persistence), not spike biology per se, often on top of prior spike-mRNA exposure already distributed across the global population. The shared risk-bearing architecture of the two payloads, and the points at which they diverge, are set out in (**Figure 6**).

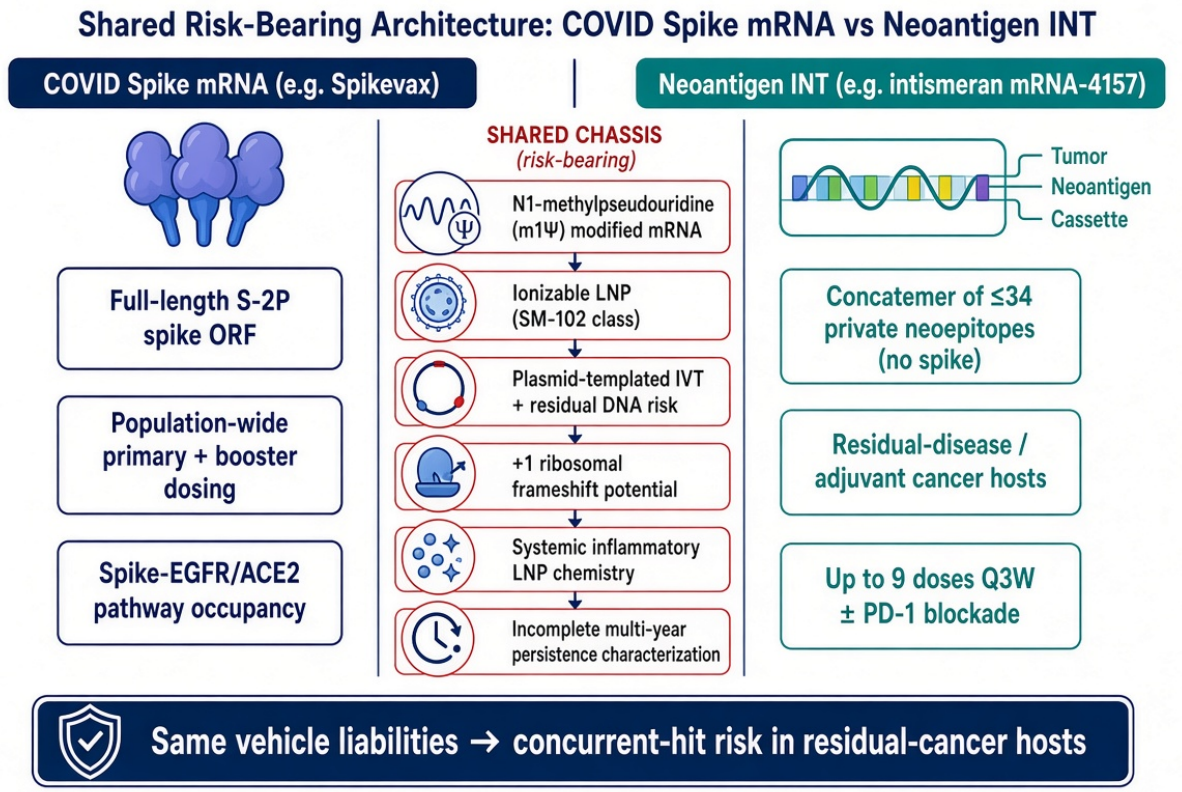

Figure 6. *Shared risk-bearing architecture: COVID spike mRNA versus neoantigen INT. Both use m1Ψ-modified mRNA, SM-102–class LNP, plasmid IVT with residual-DNA risk, frameshift potential, inflammatory LNP chemistry, and incompletely characterized multi-year persistence. Distinctions: S-2P spike ORF and population dosing versus ≤34 neoepitope concatemer (no spike) in residual-disease hosts (≤9 doses Q3W ± PD-1). Same vehicle liabilities transmit concurrent-hit risk.*

12.2 Why Residual-Disease Patients Are the Highest-Risk Recipients

Although the neoantigen payload is rationally preferred to a universal viral glycoprotein, deployment of the same nucleoside-modified mRNA–LNP chassis into adjuvant oncology concentrates risk in precisely the hosts the concurrent-hit model identifies as most vulnerable [77–82,89]. A full intismeran course comprises up to nine intramuscular 1 mg doses every three weeks—repeated inflammatory LNP and modified-mRNA exposures over approximately six months—in patients defined by resected high-risk disease and therefore by residual microscopic risk [82,83]. **Table 3** maps shared versus payload-specific liabilities. In residual-disease hosts already carrying prior spike-mRNA pathway stress, serial LNP re-challenge is not a theoretical hazard—it is a foreseeable amplifier of concurrent hits. Withdrawal of the chassis from broad and expanded use is the proportionate regulatory response until those amplifiers are independently measured and ruled out.

First, translational fidelity risk scales with ORF complexity. A concatemer encoding up to 34 neoepitopes lengthens the message and multiplies potential slippery-sequence contexts for m1Ψ-dependent +1

frameshifting [48,65]. Frameshifted polypeptides in a residual-cancer host are not merely off-target immunogens; they expand the intracellular proteomic ensemble under conditions of ribosomal and proteasome stress already linked to MYC-high post-exposure transcriptomes [12,48]. Second, manufacturing remains plasmid-templated IVT with LNP encapsulation "similar to the previously described Spikevax LNP" [82]; residual DNA fragment risk and lot-to-lot (here, patient-to-patient) variability are therefore platform inheritances, not solved by personalization [27–30,82]. Third, LNP ionizable lipids are intrinsically inflammatory (IL-1β, IL-6, TLR4-linked pathways) independent of cargo [49]. Repeated dosing in the adjuvant window delivers serial inflammatory pulses to a stem-cell and micrometastatic compartment that inflammation is known to expand and epigenetically imprint [6,49,57].

Fourth, combination with PD-1 blockade (pembrolizumab) can amplify desired neoantigen-specific T cells while intensifying immune activation, autoimmunity risk, and stress on an already rewired tumor–immune PPI network [74,78]. In the concurrent-hit frame, checkpoint intensification does not cancel CSC selection under inflammatory and fidelity-impaired conditions; it can coexist with accelerated outgrowth of immune-evasive residual clones. Fifth, shared-antigen or frameshift-peptide pipeline assets reintroduce off-tumor expression risk that pure private neoantigens avoid [81]. Sixth, multi-year persistence of vaccine mRNA, protein, and plasmid elements documented after COVID products [21] has not been systematically excluded for oncology dosing schedules; if analogous persistence occurs, pathway and stemness occupancy become chronic rather than pulsed.

These concerns do not deny reported recurrence-free survival signals in selected Phase 2/3 melanoma settings [78,83]. They assert that short-term immunogenicity and RFS gains do not bound the structural liabilities of the chassis—frameshifting, residual nucleic acids, serial LNP inflammation, and uncharacterized long-horizon product fate—in residual-disease hosts. That gap is why extension of the platform into oncology strengthens the call for withdrawal pending independent multi-omic resolution of fidelity, residuals, persistence, CSC/metastatic competence, and progression endpoints [10,12,21,48,49].

Liability domain	COVID spike mRNA (e.g., Spikevax)	Neoantigen INT (e.g., intismeran)	Refs
Encoded ORF	Full-length S-2P spike	Concatemer of ≤34 private neoepitopes; no spike	[13–16]
Nucleoside chemistry	m1Ψ; codon-optimized	m1Ψ; sequence-optimized concatemer	[48,63,64]
Delivery	Ionizable LNP (SM-102 class)	Ionizable LNP (Spikevax-similar / SM-102 class)	[31,49,60]
Manufacturing template	Plasmid IVT; residual DNA risk	Plasmid IVT; residual DNA risk; 1 lot/patient	[27,29,30]
Frameshift risk	Documented +1 frameshift products	Same chemistry; longer multi-epitope ORF multiplies contexts	[48,65]
Host context of concern	Population-wide; high-risk substrata	Residual disease / adjuvant high-risk cancer hosts	[85,86]
Dosing intensity	Primary + boosters	Up to 9 doses Q3W (~6 months) ± PD-1 blockade	[82,83]

Table 3. *Platform liabilities: COVID spike mRNA versus personalized neoantigen INT (same chassis).*

The first randomized test of this strategy without a checkpoint-inhibitor partner has now arrived, and it is a failure. In August 2026 BioNTech terminated BNT122-01 (NCT04486378), a Phase 2 trial of autogene cevumeran — an individualized mRNA neoantigen immunotherapy — given as adjuvant monotherapy

against watchful waiting in 327 patients with ctDNA-positive, surgically resected high-risk Stage II or Stage III colorectal cancer [90,91]. The population is exactly the residual-disease host this section identifies: tumor resected, adjuvant chemotherapy completed, molecular evidence of residual disease, no concurrent cytotoxic therapy. The dosing was more intensive than intismeran's — up to fifteen intravenous infusions across approximately one year [92]. The trial crossed its prespecified futility boundary in October 2025 and was continued regardless. Ten months later the independent Data Safety Monitoring Board identified a numerical imbalance in overall survival between arms, concluded that continuation was unlikely to change the efficacy outcome, and recommended termination [90].

The efficacy verdict is unambiguous. Individualized mRNA neoantigen therapy, administered as monotherapy in the setting for which it was most rationally indicated — minimal residual disease, defined molecularly, in patients with no measurable tumor to shrink — did not outperform doing nothing. The platform's central promise in oncology is that a personalized cassette can clear micrometastatic disease that surgery and chemotherapy have missed. In the first adequately powered randomized test of that promise against no treatment, it did not. The distinction from the melanoma program matters and should be stated plainly: KEYNOTE-942 tested mRNA-4157 in combination with pembrolizumab against pembrolizumab alone and reported a recurrence-free survival signal [78]. What failed in BNT122-01 is therefore the proposition that the mRNA neoantigen construct carries therapeutic benefit on its own, rather than as an adjunct to checkpoint blockade — and it is the construct, not the checkpoint inhibitor, that this review identifies as the source of risk.

Two features of the termination bear on the argument developed here. The first is the survival imbalance. BioNTech reported no new safety signals and has not disclosed the direction or magnitude of the imbalance, the event counts in either arm, the analysis population, or the data cut-off [90]. We do not assert that the treatment arm fared worse, because the data required to establish it have not been released. We observe that overall survival in a residual-disease population under repeated systemic mRNA exposure is the precise endpoint nominated as decisive in Section 17, that a randomized comparison of that endpoint has now been performed, and that the result is held by the sponsor. Publication of arm-level survival data is the single most informative disclosure available to the field.

The second feature is chemical, and it cuts against the platform rather than for it. Autogene cevumeran is uridine mRNA in a lipoplex delivered intravenously; it uses neither N1-methylpseudouridine nor the ionizable lipid nanoparticle chemistry of Spikevax and intismeran [92]. It therefore carries neither the m1Ψ-dependent frameshifting liability developed in Section 8 nor the ionizable-lipid inflammatory burden of mechanism 25. The strategy failed in residual disease without those liabilities. Intismeran proposes the same strategy, in the same host context, with them added. Nothing in the BNT122-01 outcome suggests that the m1Ψ–LNP chassis will rescue an approach that has already failed on a cleaner one, and the concurrent-hit model predicts the opposite: that appending frameshift-prone chemistry, residual plasmid DNA and inflammatory lipid to a strategy unable to demonstrate benefit moves the risk–benefit balance further toward harm, not away from it.

12.3 Off-Target Antigen Expression: Tumor Antigen Translated in Heart, Brain and Other Vital Tissue

The preceding sections address what happens when the platform's payload perturbs host signaling. A distinct hazard arises not from perturbation but from the payload performing its intended function in the

wrong compartment. It is specific to the oncology transfer, it has no analogue in the viral-antigen era of the platform, and to our knowledge it has not been measured.

Biodistribution of mRNA–LNP products is not confined to the injection site. The manufacturer's own rat program reports highest exposure at the injection site, draining lymph nodes, and spleen, with liver the highest among distal tissues and low, variable signal recovered from heart, brain, bone marrow, and gonads [31]. In humans, vaccine-derived spike antigen and vaccine mRNA have been recovered from plasma, circulating exosomes, monocyte subsets, and skin, in some cases years after dosing [21,24,25]. An autopsy series extends this to the myocardium directly: vaccine mRNA was recovered from cardiac left and right ventricle in patients dying within thirty days of dosing, and every patient with vaccine detectable in the heart showed healing myocardial injury dating to the time of the most recent injection, against 22% of those without, with significantly greater macrophage infiltration in the same ventricles [93]. Whatever the correct interpretation of trace distal signal, the operative point is that the vector, not the biology of the antigen, determines where translation occurs. A lipid nanoparticle deposits its cassette wherever it is taken up.

With a viral open reading frame, off-target translation produces inflammation and local antigen display. With a neoantigen cassette the consequence is categorically different. A non-tumor cell that takes up and translates the construct presents tumor-derived neoepitopes on MHC class I — inside a host that has been deliberately primed, over up to nine doses and under PD-1 blockade, to mount cytotoxic T-cell responses against exactly those epitopes. Such a cell is not an incidental bystander. It becomes, by the therapy's own design logic, a licensed target. The mechanism that makes the treatment work is the same mechanism that would destroy it. That sequence is traced end to end in (**Figure 7**): systemic distribution after intramuscular injection, translation and MHC-I display of the cassette in cardiomyocytes, neurons and endothelium, cytotoxic recognition of those normal cells under PD-1 blockade, and the host factors that concentrate the risk in residual-disease recipients.

This is not a speculative failure mode without precedent. In the affinity-enhanced MAGE-A3 TCR program, the first two treated patients developed cardiogenic shock and died within days of infusion; autopsy showed severe myocardial damage with T-cell infiltration, and the cause was eventually traced to cross-recognition of a titin-derived peptide presented by beating cardiomyocytes — an interaction invisible to more than thirty standard cardiomyocyte preparations and detectable only in three-dimensional iPS-derived beating culture [94,95]. In a separate MAGE-A3 program, three of nine patients developed mental status changes and two died of necrotizing leukoencephalopathy with CD3+/CD8+ infiltration of white matter, traced to previously unrecognized MAGE-A12 expression in human brain [96]. HER2-directed chimeric antigen receptor T cells produced fatal pulmonary toxicity attributed to low-level target expression on normal lung epithelium [97]. Three separate programs, three organ systems, three preclinical packages that did not predict the event.

Those precedents used engineered effector cells rather than in vivo transfection, and the analogy is not exact. What transfers is the principle, and it transfers in the direction of greater rather than lesser concern. First, target expression far below conventional detection thresholds proved sufficient to license lethal cytotoxicity. Second, the affected tissues — myocardium and central nervous system — are post-mitotic and non-regenerating, so cytotoxic loss is not replaced; a low, subclinical rate of off-target presentation could therefore accumulate as irreversible functional decrement without ever producing an acute syndrome. Third, in each case the standard preclinical screen returned a clean result. Fourth, and most directly relevant, those programs at least controlled where their effector cells were directed. An intramuscular lipid

nanoparticle does not: the encoded antigen appears wherever the particle distributes, which is a property of the formulation rather than of the construct.

If the hazard is real, its severity should not be uniform across tissues. It should track inversely with regenerative capacity, because the injury in question is cell loss, and a tissue that can replace lost cells absorbs that injury while a tissue that cannot accumulates it. That gradient organizes the predicted consequences set out below.

At the recoverable end sit the tissues with the highest measured distal exposure. Hepatocytes are the most exposed non-lymphoid population in the manufacturer's own rat data, at roughly 3% of injection-site levels [31]; hepatocytes divide, and the predicted phenotype — immune-mediated hepatitis — is one that resolves in most patients and is already a recognized checkpoint-inhibitor toxicity. Vascular endothelium is different in kind rather than degree: it is the one compartment guaranteed continuous contact with circulating particles, and cytotoxic attack there would not be organ-confined but would present as distributed microvascular injury, endothelialitis, and thrombotic propensity. Hematopoietic progenitors occupy an intermediate position — the marrow regenerates, but the stem-cell pool is finite and depletion compounds, so the predicted phenotype is cytopenia with cumulative reserve loss rather than a single reversible event.

Gonadal tissue is a special case, and the one instance where the hazard is not off-target at all. Cancer-testis antigens are so named because they are constitutively expressed in germline tissue; a shared-antigen cassette directed at MAGE-A, NY-ESO-1, or related families instructs the immune system to attack cells that normally display those epitopes, and testis lies within the measured biodistribution envelope [31,81]. For that class of construct, germ-cell injury is a predicted on-target consequence rather than an off-target accident.

The irreversible end of the gradient is where the documented fatalities occurred. Cardiomyocytes are essentially post-mitotic: carbon-dating of human myocardium places annual turnover near 1% at age 25, falling to roughly 0.45% by age 75, with fewer than half of all cardiomyocytes exchanged across a normal lifespan [98]. Cytotoxic loss is therefore not replaced by myocyte but by fibrous scar. The predicted sequence is therefore myocyte dropout, replacement fibrosis, loss of contractile reserve, and an arrhythmogenic substrate at scar borders — a trajectory that requires no acute clinical event at any point and would be invisible to a trial measuring recurrence-free survival. That the platform reaches myocardium is not speculative: post-vaccine myocarditis with free circulating spike is documented [23], and spike protein has been identified within cardiac tumor cells, tumor endothelium and tumor-associated macrophages in post-COVID resection specimens against spike-negative pre-pandemic controls [99]. More directly, isolated adult ventricular cardiomyocytes take up mRNA–LNP and translate the encoded spike within 48 hours, after which mRNA-1273 produces arrhythmic and irregular contraction with disordered calcium transients consistent with ryanodine-receptor dysfunction, and BNT162b2 produces sustained protein kinase A activation; by 72 hours the proportion of regularly contracting myocytes had fallen to near zero and to 27% respectively, and the same constructs were recovered from every region of ex vivo perfused heart [100]. The point that matters here is not the specific dysfunction but the demonstrated competence of the compartment: cardiomyocytes internalize the particle, translate the cassette, and display its product. Whether that product is viral spike or a tumor neoepitope is a property of the payload, not of the tissue. This is also the compartment in which the titin cross-reaction proved fatal within days [94,95], and in which PD-1 blockade withdraws the tolerance brake that normally restrains low-avidity self-reactive clones [101].

The central nervous system is the least forgiving compartment of all. Neurons do not divide; oligodendrocytes regenerate poorly; and the tissue tolerates lymphocytic infiltration badly even when the target is legitimate. Predicted phenotypes differ by which cell presents the cassette: neuronal presentation would produce focal deficits and cumulative cognitive decline, oligodendrocyte presentation a demyelinating syndrome, and cerebrovascular endothelial presentation barrier breakdown with neuroinflammation. This is not extrapolation from first principles alone. It is the compartment in which unrecognized MAGE-A12 expression produced fatal leukoencephalopathy [96]. Spike protein and vaccine mRNA have separately been localized to brain tissue and to the skull–meninges–brain axis, and spike protein has been demonstrated in cerebral arterial walls after mRNA vaccination, indicating that the platform's products do reach this compartment in some recipients [102].

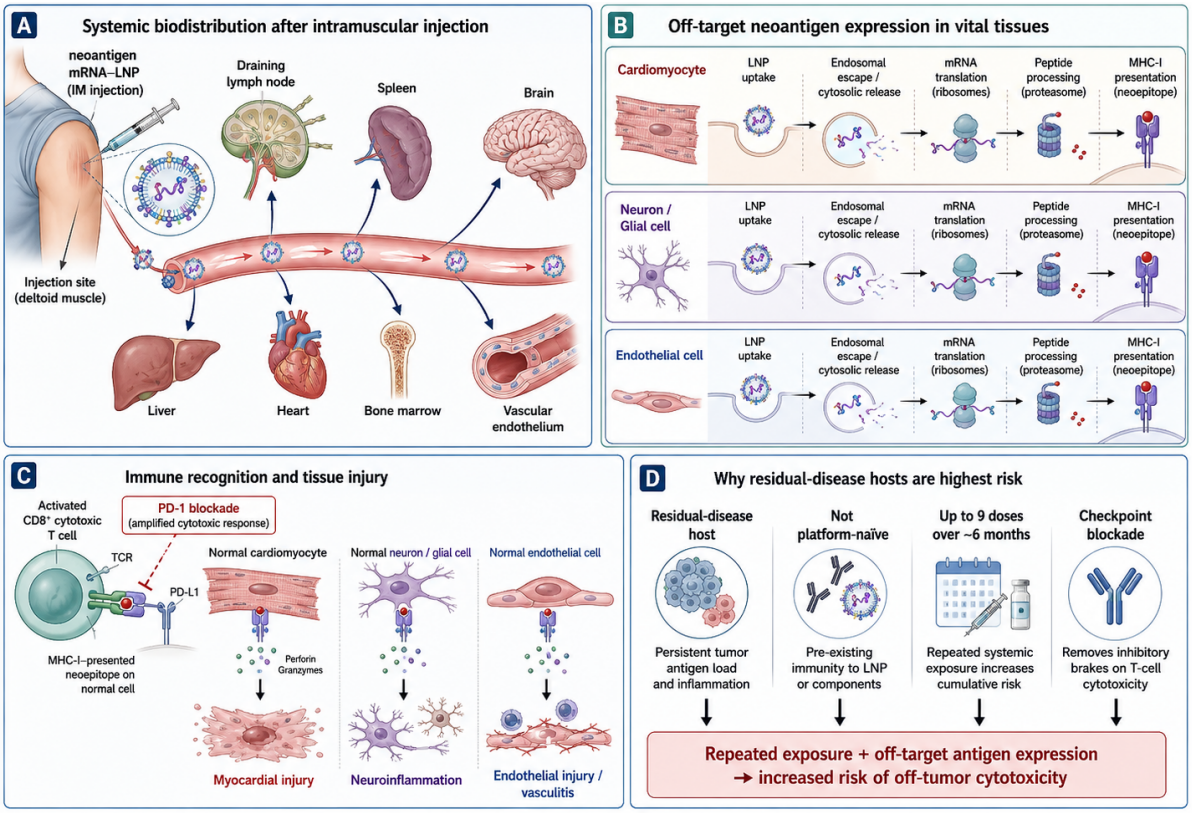

Figure 7. *Off-target biodistribution and cytotoxic consequences of neoantigen mRNA–LNP in vital tissues. (A) After intramuscular injection, lipid nanoparticles distribute beyond the deltoid to draining lymph nodes, spleen, liver, heart, bone marrow, brain, and vascular endothelium. (B) In cardiomyocytes, neurons and glia, and endothelial cells the same sequence proceeds in each cell type: LNP uptake, endosomal escape and cytosolic release, ribosomal translation of the cassette, proteasomal peptide processing, and display of the encoded neoepitope on MHC class I. (C) An activated CD8+ cytotoxic T cell primed against those epitopes engages the MHC-I–neoepitope complex on a normal cell and releases perforin and granzymes; PD-1 blockade removes the inhibitory brake that would otherwise restrain the response. Predicted phenotypes are myocardial injury, neuroinflammation, and endothelial injury or vasculitis. (D) Four features concentrate this risk in adjuvant oncology recipients: persistent tumor antigen load and inflammation in residual-disease hosts, prior exposure to the platform, up to nine doses over roughly six months, and concurrent checkpoint blockade.*

Two features make these predictions worse rather than better on repetition. Because the therapeutic objective is to break tolerance rather than to preserve it, there is no physiological off switch: an antigen-specific memory population, once established, persists and can be re-engaged by any subsequent

presentation of the same epitopes. And because the adjuvant schedule delivers up to nine doses over roughly six months, any low-level off-target presentation is not a single event but is re-primed repeatedly across the course. Epitope spreading would widen the target set further, extending reactivity past the encoded cassette to whatever else a damaged tissue releases. A rate of off-target expression far too low to produce an acute syndrome could still, under those conditions, generate measurable attrition in tissues that cannot rebuild.

We state this as a structural prediction rather than a demonstrated harm, and it is falsifiable. The relevant experiments are neither exotic nor expensive: cassette-specific RT-qPCR of non-lymphoid tissue at necropsy in the dosing species; MHC class I immunopeptidomics of myocardium, brain, and endothelium after administration, searching directly for cassette-encoded epitopes; serial high-sensitivity troponin and neurofilament light chain across the full nine-dose schedule in trial participants; and immunohistochemistry for cassette-encoded epitopes at autopsy in any recipient dying of cardiac or neurologic cause. None of these has been reported. The biodistribution package that would detect off-target antigen presentation was not designed to look for it, and the clinical program measures recurrence-free survival rather than the compartment in which the antigen is expressed. Until that gap is closed, the safety of delivering tumor-antigen templates by a systemically distributing vector into post-mitotic tissue is assumed rather than established.

13. What Emergency Authorization Did Not Measure

Emergency authorization prioritized neutralizing titers and severe-disease endpoints. Multi-year persistence, finished-product residual-DNA fragment profiling, frameshift proteomics, and lot-linked cancer-registry endpoints were not preconditions of scale-up [9,27–30,33]. Independent reports of frameshift immunity, multi-year product detection, and residual plasmid elements were met more often with method disputes and population-level reassurance than with mandatory transparent lot-level molecular disclosure [12,27,33,48,72]. Passive pharmacovigilance cannot resolve rare, delayed, multi-omic outcomes. Intended proteomic output was a single clean, briefly expressed antigen; observed ensembles include frameshifted polypeptides, residual nucleic acids, prolonged circulating antigen, exosomal broadcast, and ribosomal/proteasome stress. That gap is the operational definition of proteomic failure for this platform. Because none of these endpoints was gated before scale-up, the question of whether the platform carries oncologic risk has had to be answered after deployment, from registry data gathered for other purposes. That evidence is examined next.

14. Population-Level Cancer Signals After Vaccination

If the mechanisms developed above operate in human populations, they should leave a signature in registry data — concentrated in susceptible hosts, expressed as compressed time-to-presentation rather than uniform excess incidence. Genome instability, altered DNA repair, and LINE-1/reverse-transcription findings map to mutation pressure [10,44–46]. Oncogenic pathway activation (EGFR–RAS–MAPK, PI3K–AKT, STAT3–MYC), renin–angiotensin dysregulation, and treatment resistance (including p53-pathway interference) map to protooncogene activation and suppressor-edge loss [3,35–42,44,88]. Chronic LNP/spike inflammation, tumor-microenvironment remodeling, microbiota disruption, and immune dysregulation (including IgG4 class switch after repeated dosing) map to PPI cross-cluster rewiring and inflammatory stem-cell selection [6,11,32,49,88]. Immune evasion, impaired surveillance, and awakening of dormant clones map directly to CSC acceleration and metastatic competence in residual-disease hosts [8,9,11,43,57,88]. Frameshifted polypeptides, residual plasmid DNA, and SV40-sequence contamination

are platform structural liabilities that expand the proteomic and nucleic-acid ensemble beyond the intended antigen [27–30,48,88]. Multiple injections intensify cumulative exposure. None of these pathways alone proves population causation; their concurrent occupancy is the mechanistic basis for accelerated progression signals observed in cohort and registry data [85–87].

Four bodies of evidence now bear on that prediction: two exposure-stratified cohorts, a systematic review of the case literature, and national registry mortality data. In a 30-month province-wide Italian cohort of 296,015 residents aged ≥11 years (Pescara; June 2021–December 2023), receipt of ≥1 SARS-CoV-2 vaccine dose was associated with a higher adjusted hazard of hospitalization for any cancer versus the unvaccinated (HR 1.23; 95% CI 1.11–1.37) [85]. The association was concentrated among those without prior documented infection (HR 1.31; 95% CI 1.16–1.47) and included elevated hazards for colorectal (HR 1.34), breast (HR 1.54), and bladder (HR 1.62) cancer [85]. When the minimum lag from vaccination to hospitalization was extended to 12 months, the overall cancer signal attenuated or reversed—compatible with acceleration of clinically apparent disease into an intermediate window rather than (or in addition to) de novo initiation over longer horizons [85].

The largest of these analyses is also the most granular, and on several axes the most informative. Kim et al. examined 8,407,849 individuals in the Korean National Health Insurance Service database between 2021 and 2023 — a cohort roughly twenty-eight times the size of the Italian province study — and measured cancer incidence directly rather than hospitalization as a proxy [86]. Using propensity-score matching and multivariable Cox proportional hazards models, the authors reported statistically significant one-year elevations across six cancer types: thyroid (HR 1.35; 95% CI 1.21–1.51), gastric (HR 1.34), colorectal (HR 1.28), lung (HR 1.53), breast (HR 1.20), and prostate (HR 1.69) [86]. Three features bear directly on the concurrent-hit model. First, the associations were platform-resolved: mRNA products were linked to thyroid, colorectal, lung, and breast cancer; cDNA/adenoviral products to thyroid, gastric, colorectal, lung, and prostate cancer; and heterologous schedules to thyroid and breast cancer — a structure consistent with a shared spike-antigen component plus platform-specific increments, rather than a single undifferentiated exposure effect.

Second, booster-dose stratification identified additional elevations for gastric and pancreatic cancer, the signature expected of cumulative rather than single-exposure dependence. Third, effect modification by sex and age was evident, consistent with a mechanism whose expression depends on host substratum rather than acting uniformly across recipients. Site specificity, platform resolution, and dose dependence are precisely the features a concurrent-hit mechanism predicts and that an undifferentiated confounding artifact does not readily generate. A peer-reviewed commentary has questioned the index-date construction, in which vaccinated individuals are indexed at vaccination and unvaccinated individuals at a fixed calendar date [103]. That criticism bears on the magnitude of the point estimates rather than on their direction, and it does not account for the structure of the findings: an indexing artifact is undifferentiated by construction and does not generate platform-specific patterning, dose-stratified escalation, and effect modification by sex and age simultaneously. The Korean cohort therefore specifies which sites, which platforms, and which dose strata warrant targeted replication.

A systematic scoping review published in January 2026 assembled this literature and placed both cohorts above within it, alongside a third population-level dataset: a longitudinal analysis of approximately 1.3 million US military service members spanning the pre-pandemic through post-pandemic periods [104]. The case-level component of that review is treated separately in Section 15. The military cohort is methodologically notable because a Department of Defense mandate produced near-universal vaccination

and therefore a structured pre- and post-exposure comparison within a single, closely surveilled population: a roughly 50% rise in specified and unspecified non-Hodgkin lymphoma subtypes from 2021, with persistently elevated mature T/NK-cell lymphoma incidence relative to pre-pandemic years [105]. Those authors did not attribute the change to vaccination, and the time-trend design cannot support individual-level causal inference [104,105]. The mandate is nonetheless what makes the observation difficult to dismiss: where vaccination is near-universal and compulsory, the healthy-vaccinee selection that confounds voluntary-uptake cohorts cannot operate, and the population is under continuous medical surveillance before and after exposure. The rise is therefore observed in the setting least hospitable to the usual explanations.

In parallel, National Cancer Institute SEER incidence data record a sharp acceleration in early-onset disease across the period of mass mRNA deployment. Among Americans under age 50, incidence of all cancers combined rose from 109.45 to 116.42 per 100,000 between 2021 and 2023 — a 6.4% increase in two years [87]. The site-specific pattern is steeper still. Non-malignant brain and nervous-system tumors rose from 6.72 to 8.03 per 100,000 (+19.5%); colorectal cancer from 9.62 to 11.49 (+19.4%); small-intestine cancer from 0.71 to 0.82 (+15.5%); ovarian cancer from 4.21 to 4.75 (+12.8%); stomach cancer from 1.65 to 1.77 (+7.3%); and female breast cancer from 49.95 to 51.75 (+3.6%) [87]. Early-onset incidence had been drifting upward for years before 2021, but the post-2021 slope is a departure from that drift rather than a continuation of it, and it coincides with mass mRNA rollout beginning in late 2020. The site distribution is also not arbitrary with respect to the exposure-stratified cohorts: colorectal cancer shows the second-largest early-onset increase here and is independently elevated in both the Italian (HR 1.34) and Korean (HR 1.28) analyses, so three datasets on three continents, using three different endpoints, converge on the same organ. **Figure 8** plots these trajectories against the full 2000–2023 series.

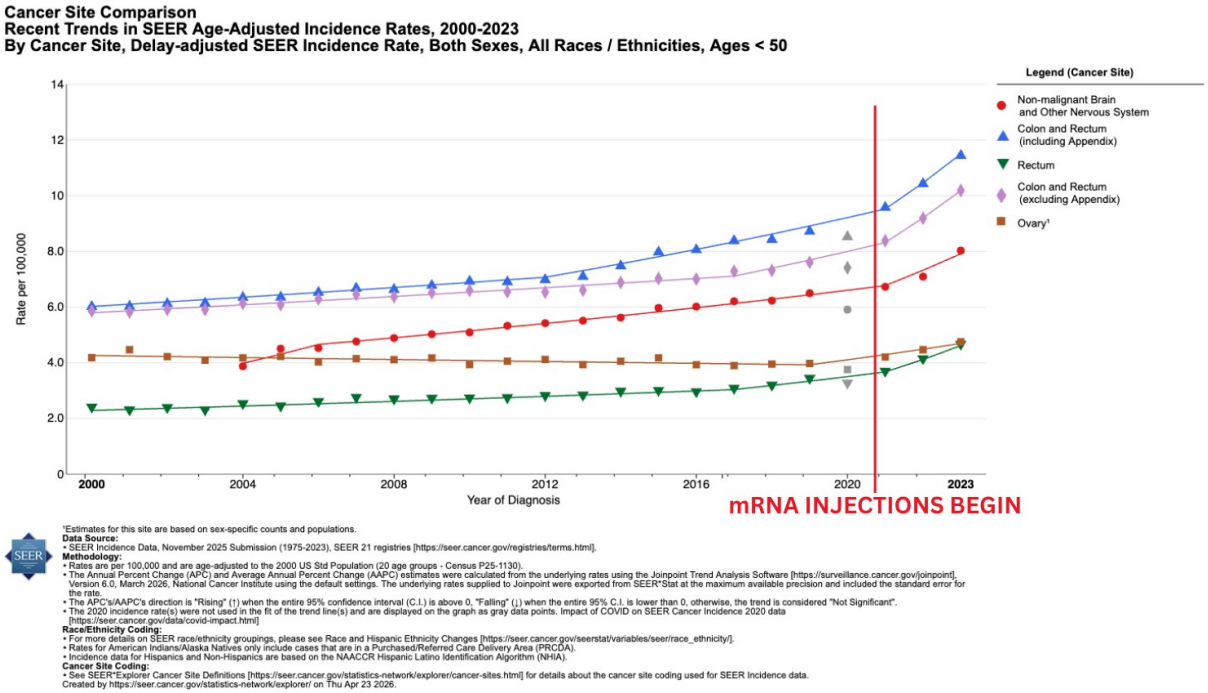

Figure 8. *Early-onset cancer incidence in the United States, 2000–2023. Delay-adjusted, age-adjusted SEER incidence per 100,000 for both sexes, all races and ethnicities, ages under 50, from SEER Incidence Data, November 2025 Submission (1975–2023), SEER 21 registries; rates are age-adjusted to the 2000 US standard population and trend lines were fitted by Joinpoint. The 2020 rates were excluded from trend fitting because of pandemic-related disruption to diagnosis and are shown as grey points. The vertical line marks the beginning of mass mRNA vaccination. Against two decades of gradual drift, colorectal and non-malignant brain and nervous-system tumors both inflect sharply after 2021, the two sites with the largest early-onset increases reported in the text [87].*

An independent time-series analysis of CDC WONDER underlying-cause mortality reports excess cancer mortality near 10% ($z \approx 15$) against a 2014–2019 baseline, a shift in the compound annual growth rate of cancer mortality from approximately 0.23% to 1.8%, and a 44% excess (17-sigma) confined to the 0–54 age bracket, with the inflection placed at Morbidity and Mortality Weekly Report (MMWR) week 14 of 2021 — the standard CDC surveillance week running 4–10 April 2021, and the week of peak US mRNA vaccine uptake [106]. Two features of that analysis bear on how the signal has been read. Cumulatively, 154,330 excess cancer deaths have been recorded since the Week 14, 2021 inflection (z-score = 15), currently running at approximately 949 per week against the 2014–2019 baseline. A further 531 cancer deaths per week are reassigned out of the underlying cause-of-death field and onto multiple cause-of-death lines in excess of pre-pandemic practice — deaths that must be added back before post-2021 cancer mortality is comparable to its own historical baseline at all [106]. Underlying-cause tabulations that omit this correction therefore understate the excess by roughly a third, which is one reason the signal has been reported as absent in analyses drawing on raw underlying-cause data [106]. Registry-wide mortality data cannot stratify by individual vaccination status, but the same analysis reports a geographic gradient that partially substitutes for it: excess cancer mortality runs approximately twofold higher in the most heavily vaccinated U.S. states than in the least [106]. A purely temporal artifact of the pandemic period would not be expected to sort by state-level vaccine uptake. **Figure 9** plots the same mortality series compiled directly from federal files, in which the timing of the inflection and the sustained departure from the pre-vaccine trend are visible against a baseline that is a simple linear extrapolation of the 2015–2019 series [107,108].

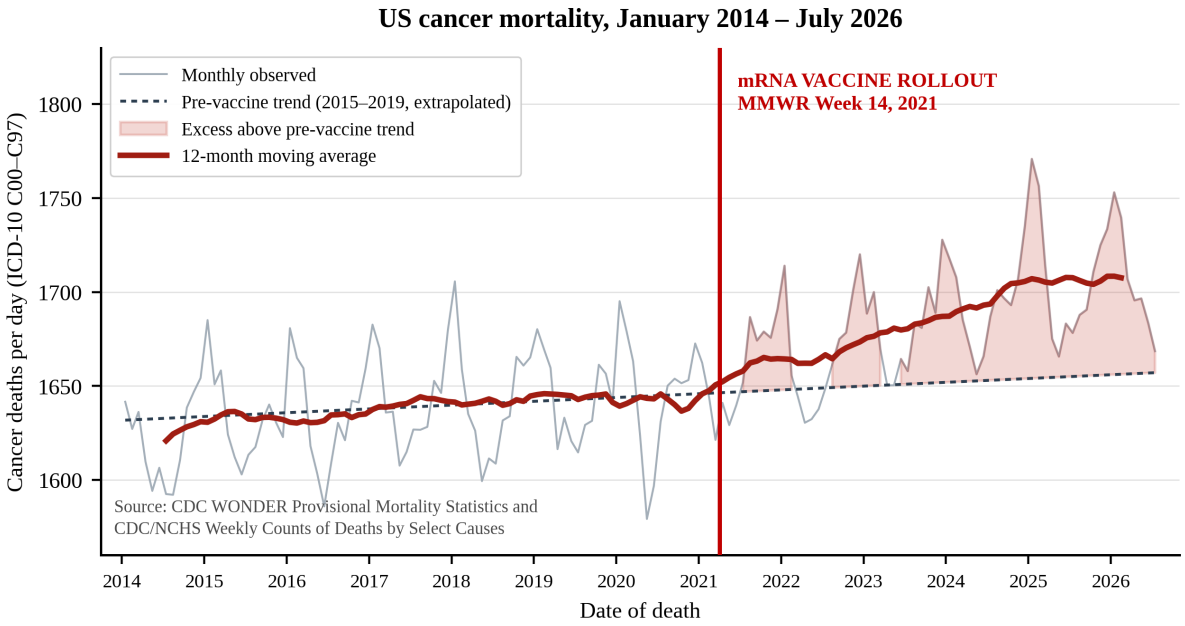

Figure 9. *United States cancer mortality, January 2014 to July 2026. Deaths with malignant neoplasm (ICD-10 C00–C97) as underlying cause, compiled by the present authors from two federal sources: CDC/NCHS Weekly Counts of Deaths by State and Select Causes for 2014–2017 and CDC WONDER Provisional Mortality Statistics for 2018 onward [107,108]. All values are expressed as deaths per day, and the weekly counts are collapsed to monthly means, so that both halves of the series carry the same sampling interval and are directly comparable; the two sources agree to within 0.02% across their period of overlap. The heavy line is a 12-month moving average, the dashed line extrapolates the 2015–2019 pre-vaccine trend, and shading marks observed mortality above that trend. The red rule marks MMWR week 14 of 2021 (4–10 April 2021), the week of peak US mRNA vaccine uptake. August 2026 is omitted as incomplete. Cancer mortality was close to flat across the pre-vaccine period, rising 0.16% per year between 2015 and 2019; from the 2021 inflection the series departs from that trend and has not returned to it. The figure is presented to show the timing and shape of the signal in observed federal counts against a baseline that is a plain linear extrapolation of the stated pre-vaccine years, with no pull-forward or coding adjustment of any kind; quantified excess mortality is given in the text.*

Given the weight this estimate carries, we sought to verify it independently from the primary federal files. Two CDC WONDER queries were run: underlying-cause deaths with malignant neoplasm (C00–C97) as the coded cause, and multiple-cause deaths with C00–C97 recorded anywhere on the certificate, both grouped by month [107,109]. Historical multiple-cause data were drawn from the final 1999–2020 file and the provisional file thereafter; the two agree exactly across their 36-month overlap. A baseline was fitted to the six pre-pandemic years 2014–2019 and extrapolated forward. That baseline rises at 0.23% per year, reproducing exactly the annual growth rate reported in the published analysis [106] and confirming that both calculations proceed from the same reference.

The underlying-cause component is straightforward. Measured against the extrapolated 2014–2019 trend, deaths recorded with malignant neoplasm as underlying cause exceed expectation by 47,012 between April 2021 and July 2026, approximately 169 per week. This is the component displayed in **Figure 9**, which plots the observed series against that same baseline with no further adjustment of any kind.

The coding component is larger, and our derivation confirms the phenomenon the published analysis identifies [106]. The gap between multiple-cause and underlying-cause cancer deaths — certificates on which cancer is recorded as contributing but another condition is coded as the killer — widened modestly before the pandemic, from 152.7 per day in 2014 to 178.6 per day in 2019, then stepped sharply to 228.1

per day in 2020, peaked at 249.1 in 2022, and stands at 237.9 in 2026. Deaths are therefore being removed from the underlying-cause cancer tabulation at a rate far above the historical norm, exactly as reported [106]; underlying-cause counts alone understate cancer mortality against its own baseline, and the correction the published analysis applies is warranted. Charging the excess only against the pre-pandemic trend in the gap itself — the most restrictive assumption available — yields 72,118 reassigned deaths since April 2021, approximately 259 per week, against the 531 per week reported [106]. Combining components gives 119,130 excess cancer deaths, about 428 per week: an independent calculation, from raw federal data and by a different analytic route, that recovers 77% of the published total [106] and establishes a firm floor beneath it.

The remaining difference is explained, and it favors the published estimate [106]. Our calculation makes no allowance for mortality displacement — the pull-forward of deaths among people already gravely ill, including cancer patients, who died of COVID-19 and would otherwise have died of cancer inside the observation window. Displacement of this kind depresses the true counterfactual below the pre-pandemic trend, so a calculation that omits it, as ours does, necessarily understates excess mortality. The published analysis incorporates such a correction [106], and on plausible parameters — approximately 1.2 million US COVID-19 deaths, 8–10% with cancer recorded, and 35–65% of those who would have died of cancer within the window — the pulled-forward deficit falls between 33,600 and 78,000 deaths. Applied to our floor, this places the corrected total between roughly 153,000 and 197,000. The published figure of 154,330 [106] sits at the lower bound of that interval, which indicates that it is not an overstatement but a conservative reading of the available data. One feature of the reassignment deserves note: it begins in 2020, so pandemic certification practice contributed to its onset. What that explanation does not account for is its persistence. A purely COVID-driven coding artifact should have decayed as COVID-19 mortality fell; instead the gap remains 27.9 deaths per day above the extrapolated pre-pandemic trend in 2026, a departure of 2.5 standard deviations, five years after the inflection and long after COVID-19 deaths returned to low levels.

These documented patterns align with the concurrent-hit prediction of compressed time-to-clinically-evident disease—higher short- to intermediate-term hospitalization or diagnosis rates in exposed cohorts, site heterogeneity, and sensitivity to lag-time definitions—especially where residual disease, DNA-repair vulnerability, or stem-cell pools already exist [10,12,85,87]. Italian lag-time sensitivity is particularly informative for the acceleration (versus pure initiation) hypothesis, and the direction of the attenuation matters more than its existence. An early-concentrated excess that merely fades is equally compatible with ascertainment bias, since vaccination brings recipients into clinical contact. What ascertainment bias cannot generate is a signal that falls below unity at long lag: finding cases earlier does not remove them from the later window. A reversal requires that the susceptible pool be depleted — that events have been pulled forward rather than merely detected sooner — which is the specific signature of accelerated presentation and not of surveillance intensity. The Italian analysis reports exactly that attenuation-or-reversal behavior, and it is the feature most worth resolving in replication [85]. Taken together with persistence, frameshift, residual-DNA, MYC/stemness, and PPI evidence, the population signals reinforce the authors' call for platform withdrawal pending transparent, lot-linked, multi-omic and registry-grade resolution of progression and incidence endpoints [21,48,85–87].

15. Case-Level and Tissue-Level Evidence

Registry data can establish whether exposed populations experience more cancer; it cannot establish what that cancer looks like. The concurrent-hit model makes predictions that are histological and anatomical rather than epidemiological — accelerated progression of disease that was previously indolent or controlled, involvement of the injection site and its draining nodes, and the presence of vaccine-derived product inside tumor tissue. Those predictions are resolvable only at the level of the individual case. The case literature is therefore not a weaker substitute for cohort data; it is the only evidence tier in which the model's distinctive claims can be observed at all.

The scoping review introduced above assembled that literature systematically, and its composition is itself informative. Screening publications from January 2020 through October 2025 against prespecified eligibility criteria, Kuperwasser and El-Deiry identified 69 publications describing 333 patients across 27 countries [104]. The vast majority of these cases occurred following COVID-19 vaccination, with a minority following SARS-CoV-2 infection. The evidence base is dominated by direct clinical observation: 50 single-patient case reports (72%), 5 case series (7%), 8 cohort or population-level analyses (12%), 3 systematic or narrative reviews (4%), and 3 mechanistic or translational studies (4%) [104]. Reporting is geographically dispersed rather than clustered in any one surveillance system — Japan and the United States contributed 11 publications each, China 7 and Italy 4, with further reports from Spain, South Korea, Saudi Arabia, India, Nigeria, Brazil, Turkey, Singapore, Lebanon, Egypt, Bulgaria, Taiwan, Ukraine, Iran, Russia, Greece, Austria, Germany and Poland [104]. The same phenotype is therefore being described independently across diverse healthcare systems and diagnostic infrastructures.

The platform distribution is the most direct finding for the argument of this review. Among the vaccine-associated reports, roughly 86% followed nucleoside-modified mRNA–LNP exposure: approximately 56% after Pfizer-BioNTech (BNT162b2), 25% after Moderna (mRNA-1273), and a further 5% in patients who received both products across different doses [104]. All other platforms combined account for the remainder — adenoviral vectors about 10% (ChAdOx1 5.8%, Ad26.COV2.S 2.9%, Sputnik-V 1.4%) and inactivated vaccines 2.6%. Deployment share is the obvious objection to reading anything into that ratio, and the review's authors raise it themselves. It is answered by the one dataset in this literature equipped to test platform specificity: the Korean national cohort, which is exposure-stratified and comparator-controlled, found the elevation concentrated in mRNA recipients with dose-dependent escalation [86]. Where the question can be tested against a denominator, the mRNA platform is where the risk sits. The case series and the cohort point the same way.

The malignancy distribution is not random with respect to the mechanisms developed in Sections 4 through 7. Lymphoid malignancies are the single largest category at 43% of publications (30/69), spanning diffuse large B-cell lymphoma, angioimmunoblastic and subcutaneous panniculitis-like T-cell lymphomas, chronic lymphocytic leukemia/small lymphocytic lymphoma, and cutaneous T-cell lymphomas [104]. Solid tumors follow at 41% (28/69) — melanoma, breast, lung, glioblastoma and other glial tumors, sarcomas, and pancreatic carcinoma — with the remaining 16% (11/69) unspecified or mixed. That lymphoid predominance is the expected distribution if the initiating insult acts on the immune compartment: it is the same compartment in which IgG4 class switching, lymphopenia, and cytotoxic T-cell exhaustion have all been documented after repeated dosing [9,32,34]. Virus-associated malignancies — Kaposi sarcoma, Merkel cell carcinoma, and EBV-positive lymphomas including EBV-positive nasal-type NK/T-cell lesions — recur throughout the series [104]. These are the cancers whose emergence is gated by immune surveillance rather than by mutational burden, and their appearance is a recognized clinical readout that

surveillance has failed. Glioblastoma and pancreatic adenocarcinoma, by contrast, are the tumors for which the reports most consistently describe unusually rapid onset, short-latency recurrence, and aggressive progression atypical for those diagnoses [104].

The anatomical distribution is more specific still, and it is the finding least explicable by deployment share or reporting bias. A subset of reports describe tumor formation or recurrence at or near the vaccine injection site, in the deltoid region, in the axilla, or in draining lymphatic basins, including cases in which axillary lymphadenopathy coincided with solid-tumor metastasis [104]. Within the lymphoma series the pattern is explicit: T-cell lymphomas were dominated by cutaneous and follicular-helper-derived entities with several arising at injection sites, and B-cell lymphomas were characterized as primarily diffuse large B-cell, often nodal or axillary following mRNA vaccination, and typically de novo rather than transformed from prior indolent disease [104]. A malignancy arising in the deltoid or its draining nodal basin, in the weeks after an intramuscular injection into that deltoid, is an anatomical coincidence that deployment share cannot produce. It is precisely the localization the concurrent-hit model predicts if the initiating exposure is delivered intramuscularly, drains regionally, and persists.

Three recurrent themes emerged across the reports, and each maps onto a specific element of the model [104]. The first is unusually rapid progression, recurrence, or reactivation of preexisting indolent or controlled disease — the compressed time-to-presentation that concurrent rather than sequential hits predict. The second is atypical or localized histopathology, including involvement of vaccine injection sites and draining lymph nodes — the anatomical signature expected when the initiating exposure is delivered intramuscularly and drains regionally. The third is an immunologic link to tumor dormancy, immune escape, and microenvironmental shift — the dormancy-escape step developed in Section 7. These themes were identified inductively, by authors cataloging what clinicians had reported, without reference to the framework advanced here; that they reproduce three of its central predictions is not a coincidence the model was constructed to accommodate.

Two reports move beyond temporal association to place vaccine-derived antigen inside tumor tissue. A cutaneous metastasis of breast carcinoma arising within one month of a sixth BNT162b2 dose stained positive for spike protein and negative for nucleocapsid [110]. That combination is the discriminating one: nucleocapsid is produced by infection but not encoded by the vaccine, so spike-positive, nucleocapsid-negative tumor tissue indicates vaccine-derived rather than infection-derived antigen. A separate cardiac tumor series bears on the same question from the infection side. Among 173 heart tumors analyzed at a single center between 2016 and 2023, spike protein was detected by immunohistochemistry in 10 of 11 tumors resected in the post-COVID period — within tumor cells, vascular endothelium, and CD68+ macrophages, confirmed by immunofluorescence — while none of the ten pre-2020 control myxomas expressed it, and the total number of cardiac tumors rose 1.5-fold by 2023 [99]. That series concerns infection rather than vaccination: its authors found no correlation with vaccination status, and the vaccinated subset had received Sputnik-V, Sputnik Light, or EpiVacCorona rather than any mRNA product. It therefore cannot speak to vaccine attribution. What it does establish, with a spike-negative historical control, is that spike protein localizes to and persists within tumor cells, tumor endothelium, and tumor-associated macrophages. That is a property of the antigen, not of the route by which it arrives — and the mRNA platform delivers the same antigen, endogenously translated, for a duration measured in years rather than weeks [21]. Neither report establishes that the antigen caused the malignancy. Both establish that the encoded product reaches, and is expressed within, the tumor compartment itself — which is the premise on which the receptor-occupancy and network-rewiring mechanisms of Sections 4 and 6 depend.

A third report addresses the genomic tier directly. In a case of aggressive stage IV bladder cancer following mRNA vaccination, a host–vector chimeric read was recovered from circulating tumor DNA and mapped to a non–safe-harbor locus at 19q13.42 [10]. The significance is not frequency — integration-class events are expected to be rare — but location: 19q13.42 is a gene-rich region, and the observation demonstrates that when such an event does occur it can land in an oncogenically consequential neighborhood rather than in inert sequence. It is the only human observation in this review that connects the residual-DNA and integration mechanisms of Section 8 to a specific malignancy in a specific patient.

16. Inventory of Thirty-Five Oncogenic Mechanisms

A published synthesis of more than 100 experimental, clinical, and epidemiologic reports organized at least seventeen distinct pathways by which nucleoside-modified mRNA–LNP COVID products may induce, accelerate, or unmask malignancy [88]. Consolidating that synthesis with the primary literature developed across this review yields thirty-five mechanisms that survive a stricter test: each must specify a causal path to malignancy rather than an observation, an outcome, or a harm of another kind. Applying that test excludes tissue-level antigen findings, clinical outcome signals, and the off-target cytotoxicity hazards of Section 12.3, all of which are real but are not themselves oncogenic mechanisms. These mechanisms are not thirty-five independent diseases; they collapse onto the four concurrent hits developed in this review—protooncogene activation, mutation pressure, PPI-network interference, and CSC clonal acceleration—plus the structural liabilities of frameshifting, residual DNA (including SV40 promoter elements in some lots), chronic inflammation, and impaired immune surveillance [9–12,21,27–30,35,37–39,44,45,48,49,88]. **Table 4** inventories the full set and maps each mechanism onto the concurrent-hit architecture. **Figure 10** presents the same inventory graphically, grouping each mechanism under the route it primarily serves and situating them against the systemic biodistribution that makes concurrent occupancy possible.

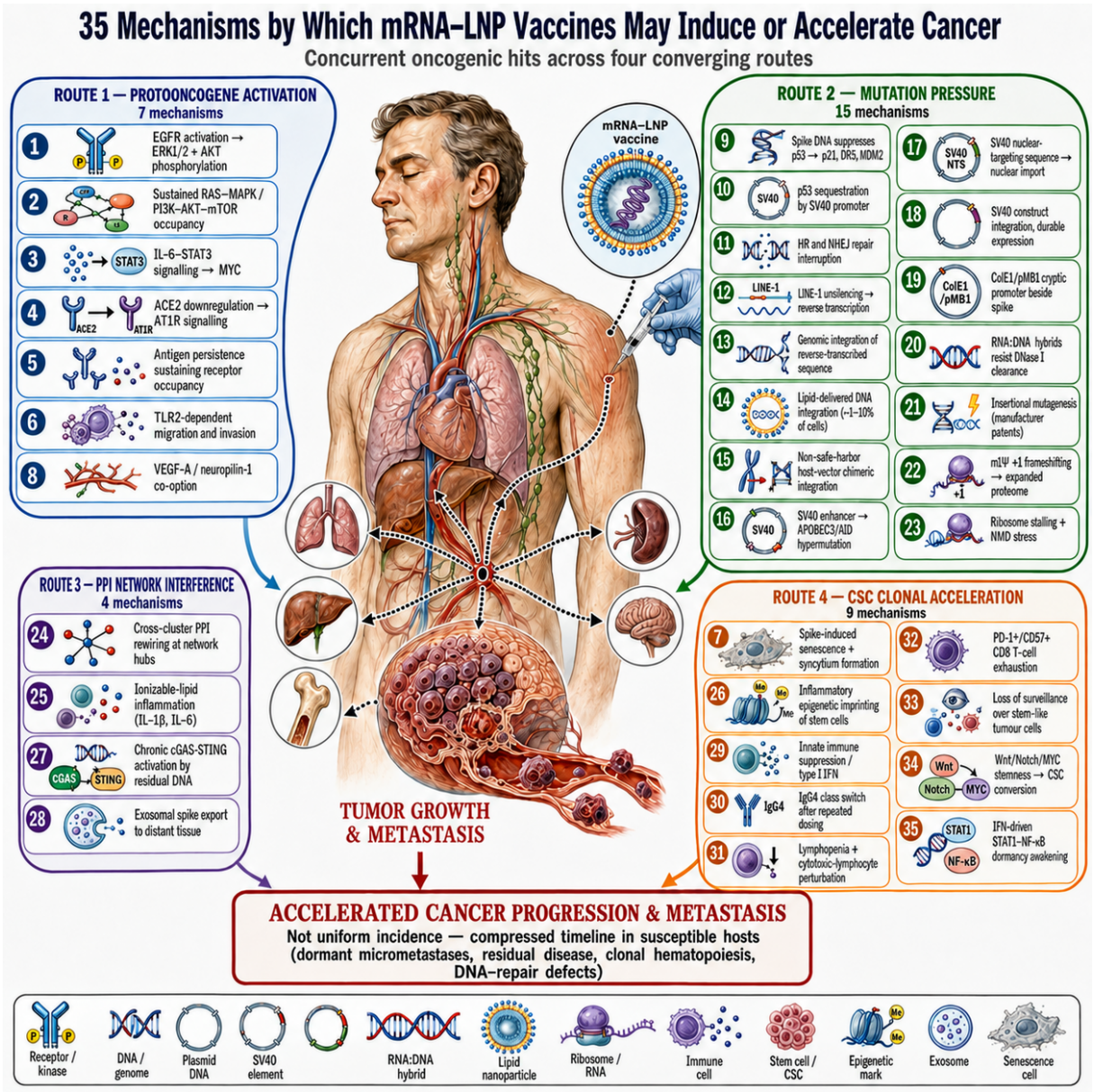

Figure 10. *Thirty-five mechanisms by which nucleoside-modified mRNA–LNP products may induce or accelerate cancer, organized by the concurrent hit each primarily serves. Route 1, protooncogene activation; Route 2, mutation pressure; Route 3, PPI-network interference; Route 4, cancer stem-cell clonal acceleration. The central panel shows systemic biodistribution after intramuscular injection, with dotted paths from the deposition site to lung, liver, spleen, brain, and bone marrow, and the predicted convergent outcome of accelerated progression and metastatic outgrowth. Numbering corresponds to* ***Table 4****. Routes are shown as discrete for clarity; twelve mechanisms feed a second route, and the full mapping is given in the Hit column of* ***Table 4****. Frameshifting and decay stress (22, 23) are grouped with mutation pressure following the concurrent-hit framework, though they act at translation rather than on DNA sequence.*

#	Mechanism	Oncogenic consequence	Refs	Hit
A. Protooncogene activation and sustained growth signaling				
1	Spike S1/RBD activation of EGFR with ERK1/2 and AKT phosphorylation at EGF-comparable magnitude	Ligand-independent proliferative drive; survivin induction blocks apoptosis	[35]	I, III
2	Sustained RAS–MAPK and PI3K–AKT–mTOR occupancy beyond physiologic ligand transit	Converts a transient growth signal into chronic proliferative signaling	[35,39]	I
3	IL-6–STAT3 inflammatory signaling converging on MYC	Induces MYC and anti-apoptotic transcriptional programmes	[3,39,43]	I, IV

#	Mechanism	Oncogenic consequence	Refs	Hit
4	ACE2 downregulation shifting renin–angiotensin balance toward AT1R signaling	Pro-proliferative and pro-angiogenic tone in exposed tissue	[39,40]	I, III
5	Antigen persistence maintaining receptor occupancy over months to years	Prevents relaxation of the rewired signaling state; sustains clonal selection	[21,24]	I, III
6	Spike protein induction of migration and invasion in lung cancer cells via TLR2, with IL-6, IL-1β and TNF-α release	Directly increases invasive and metastatic competence of existing tumor cells	[111]	I, IV
7	Spike-induced cellular senescence and syncytium formation	Senescence-associated secretory phenotype is an established tumor-promoting milieu	[112]	IV
8	Spike co-option of VEGF-A/neuropilin-1 receptor signaling	Angiogenic signaling supporting tumor vascular supply	[113]	I, IV
B. Tumor-suppressor inactivation				
9	Transfected spike DNA suppressing p53 activation of p21(WAF1), TRAIL DR5 and MDM2	Loss of cell-cycle arrest and apoptosis; survival after chemotherapy	[44]	II, III
10	p53 engagement and sequestration by SV40 promoter sequence in residual DNA	Titrates suppressor protein away from genomic targets	[54]	II, III
11	Interruption of homologous-recombination and non-homologous end-joining repair	Unrepaired lesions accumulate as driver mutations	[39]	II
C. Mutagenesis, integration and genomic instability				
12	LINE-1 unsilencing with intracellular reverse transcription of vaccine mRNA	Creates a DNA copy of the construct inside the cell	[45]	II
13	Genomic integration of reverse-transcribed sequence in human cells	Insertional mutagenesis at the integration locus	[46]	II
14	Spontaneous integration of lipid-delivered DNA in ~1–10% of transfected cells	Establishes a non-trivial per-cell probability of insertional events	[47]	II
15	Non–safe-harbor host–vector chimeric integration recovered from human malignancy	Integration into gene-rich, oncogenically consequential loci	[10]	II
16	SV40 enhancer recruitment of APOBEC3/AID cytidine deaminases	C-to-T somatic hypermutation, an established route to lymphomagenesis	[50]	II
17	SV40 nuclear-targeting sequence importing cytoplasmic DNA into the nucleus	Delivers residual DNA to the compartment where integration occurs	[51]	II
18	SV40-derived construct integration with durable transgene expression	Persistent expression from an integrated locus	[52]	II
19	ColE1/pMB1 bacterial origin acting as a cryptic mammalian promoter adjacent to the spike sequence	Aberrant transcription of adjacent integrated sequence	[53]	II
20	RNA:DNA hybrid resistance to DNase I shielding spike-encoding DNA from clearance	Preserves intact, integration-competent DNA missed by assays calibrated on naked DNA	[68–71]	II
21	Insertional-mutagenesis potential of residual plasmid DNA, with integration frequency and daughter-cell heritability acknowledged in manufacturer patent filings	Genomic alteration transmissible to progeny cells	[72,73]	II
D. Proteotoxic and translational stress				
22	m1Ψ-dependent +1 ribosomal frameshifting expanding the translated proteome beyond the intended antigen	Proteostatic burden on an already MYC-high, stress-sensitive state	[12,48,65]	II, III
23	Ribosome stalling and nonsense-mediated decay stress from modified-nucleoside translation	Chronic proteostasis stress favouring stress-tolerant clones	[48,63,64]	II
E. Network-level rewiring				
24	Cross-cluster protein–interaction rewiring at receptor, kinase, suppressor, interferon and stemness hubs	Simultaneous multi-hallmark occupancy rather than single-pathway change	[55,56]	III
F. Inflammation as a tumor-promoting enabler				
25	Ionizable-lipid intrinsic inflammatory activity (IL-1β, IL-6) independent of cargo	Sustained inflammatory milieu, an established tumor-promoting condition	[7,49,60]	III, IV
26	Inflammation-induced epigenetic imprinting of repair-activated stem cells	Expands a stem pool retaining a higher-risk state after the insult resolves	[6]	IV
27	Chronic cGAS-STING activation by residual and hybrid-protected foreign DNA	Sustained cytosolic DNA sensing, a pathway with established tumor-promoting roles	[68,114]	III, IV
28	Exosomal export of spike protein to distant tissue	Disseminates bioactive antigen beyond the injection site	[26]	III, IV
G. Immune-surveillance failure				
29	Innate immune suppression with type I interferon modulation	Reduced detection and clearance of transformed cells	[11]	IV
30	IgG4 class switch toward non-inflammatory spike-specific antibodies after repeated dosing	Blunted effector clearance and tolerance toward antigen-bearing cells	[32]	IV
31	Lymphopenia and cytotoxic-lymphocyte perturbation	Diminished cell-mediated antitumor surveillance	[9]	IV

#	Mechanism	Oncogenic consequence	Refs	Hit
32	Repeated antigen exposure driving PD-1+/CD57+ CD8 T-cell exhaustion in cancer patients, inversely correlated with IFN-γ output; also reported in post-vaccination syndrome cohorts	Diminished cytotoxic surveillance in precisely the hosts targeted for adjuvant dosing	[34,115]	IV
33	Loss of immune surveillance over stem-like tumor cells	Permits outgrowth of immune-evasive cancer stem-cell clones	[57]	IV
H. Stemness induction and dormancy escape				
34	Wnt/Notch/MYC stemness activation and conversion of pluripotent cells toward cancer stem-cell phenotype	Generates self-renewing, dissemination-competent cells	[8,57,58]	IV
35	Interferon-driven STAT1–NF-κB remodelling of the metastatic niche	Awakens dormant metastatic cells into proliferative outgrowth	[59]	IV

Table 4. *Inventory of thirty-five candidate oncogenic mechanisms of nucleoside-modified mRNA–LNP products, grouped by domain and mapped onto the four concurrent hits. Each entry states its causal path to malignancy, is referenced to a primary source, and is mapped in the final column to the concurrent hit it serves (I, protooncogene activation; II, mutation pressure; III, PPI-network interference; IV, cancer stem-cell clonal acceleration, which subsumes inflammatory imprinting and immune evasion). Twelve mechanisms carry two tags because they feed two hits; Section 6.4 identifies in-frame spike, frameshift products, residual DNA sensing, LNP inflammation, exosomal cargo export, and antigen persistence as platform-specific sources of network interference, so those entries are tagged III in addition to their primary hit. Entries that describe observations, clinical outcomes, general tumor biology, or non-oncogenic harms are excluded by design.*

17. Validation Metrics and Falsification Criteria

Domain-specific metrics can move the model from plausibility to testable status, with progression and metastasis as preferred clinical endpoints in high-risk substrata. Protooncogene activation: phospho-EGFR/ERK/AKT/STAT3 and MYC-target GSEA (FDR < 0.05) sustained weeks after exposure. Mutation pressure: TMB/indel enrichment, γH2AX/RAD51 foci, LINE-1 activity, host–vector chimeric reads with integration-site annotation, NMD/ribosomal stress signatures. PPI interference: differential interactomes of EGFR, MYC, p53, STAT3 and phosphoproteome rewiring distance. CSC acceleration and metastatic competence: ≥2× expansion of functional stem populations, single-cell stemness and invasion scores, serial sphere/organoid assays, immune-evasion co-markers within the stem cluster, and time-to-progression or distant-metastasis endpoints in matched cohorts. Platform enablers: orthogonal confirmation of product persistence, frameshift peptides or residual DNA in the same biospecimen set. Off-target antigen expression: cassette-specific RT-qPCR of non-lymphoid tissue at necropsy; MHC class I immunopeptidomics of myocardium, brain, and endothelium screened for cassette-encoded epitopes; and serial high-sensitivity troponin and neurofilament light chain across the full dosing schedule. A research-positive call in this domain requires cassette-encoded peptide recovered from a post-mitotic tissue, or a rising cardiac or neuronal injury marker tracking dose number.

A positive concurrent-hit call for research use requires ≥3 domains positive plus a platform persistence/frameshift/residual-DNA marker. Clinical enrichment of accelerated progression or early metastatic events in exposed high-risk patients, accompanied by the multi-domain molecular signature, would support the model's central prediction. Falsifiers include isolated single-domain change, full explanation by infection alone, no enrichment of rapid progression/metastasis in high-risk substrata, or disappearance of multi-domain phenotypes when frameshift-prone sequence and residual DNA are minimized in experimental systems. Pre-registered, HLA-aware, lot-linked multi-omic case–control designs with progression-free and metastasis-free survival endpoints are the minimum epidemiologic package. One randomized comparison of precisely this kind has already been performed and then stopped: BNT122-01 tested individualized mRNA neoantigen monotherapy against watchful waiting in molecularly defined residual colorectal cancer and was terminated on an overall survival imbalance that has not been quantified or attributed to an arm [90,91]. Release of those arm-level survival data would answer, in a

randomized setting, the question this section otherwise proposes to approach observationally, and is the single highest-yield disclosure now available.

18. Implications for Precision Molecular Medicine

True neoantigen therapeutics—patient-specific peptides or controlled nucleic-acid constructs selected by MHC presentation, expression, and immunogenicity—remain a rational direction. The argument is not against neoantigen science. The BNT122-01 termination sharpens rather than weakens that distinction: the strategy failed in residual disease on a uridine-mRNA lipoplex chassis that carries neither m1Ψ frameshifting nor ionizable-lipid inflammation [90,92], which indicates that the approach itself requires rethinking before the more liability-laden chassis is scaled into the same population. The argument is against deploying an inflammatory, systemically distributing, imperfectly faithful nucleic-acid vehicle into residual-cancer hosts under incomplete long-horizon characterization, and against treating pandemic-scale COVID use as sufficient safety validation for that vehicle in oncology. Platforms that minimize residual regulatory DNA, reduce frameshift-prone architecture, constrain biodistribution, and undergo prospective multi-omic surveillance in the populations they treat are more consistent with precision molecular medicine.

19. Existing Calls for Market Withdrawal

The withdrawal recommendation advanced here is not novel, and it is not isolated. It joins a body of prior calls that has accumulated steadily since the first year of deployment, and the grounds cited in those calls overlap substantially with the liabilities developed in this review. A recent compilation documents more than 81,000 physicians, scientists, researchers, and concerned citizens; 240 elected government officials; 17 professional public health and physician organizations; two state political parties; 17 county committees; and six scientific studies calling for market withdrawal of COVID-19 vaccines [116].

The organizational record begins early. Doctors for COVID Ethics called for a global recall in March 2021, and in May of that year fifty authors called for a pause in mass vaccination absent independent data safety monitoring boards, event adjudication committees, and risk mitigation. The World Council for Health issued a cease-and-desist declaration in November 2021. More than 17,000 physicians and scientists signed the Global COVID Summit declaration in May 2022. The Association of American Physicians and Surgeons called for removal in March 2023, the National Citizens Inquiry in September 2023, and New Zealand Doctors Speaking Out with Science presented a parliamentary letter in February 2024. The HOPE Accord gathered 64,168 signatories in July 2024 [116].

Peer-reviewed manuscripts have reached the same conclusion on independent grounds. Published analyses in 2024 concluded that the products are unsafe for human use and should be removed, identified a breach in the safety-signal threshold for cerebral thrombosis, recommended a moratorium on the basis of incomplete data and potential long-term risk, and called for a halt to all RNA biologicals specifically on account of residual DNA contamination — the same finished-product liability developed in Section 8 of this review [116].

Elected and regulatory actors have moved in parallel. The NORTH Group wrote to the heads of state of eleven European countries in November 2024 seeking suspension of modified mRNA vaccines; four members of the European Parliament and eight current and former Australian federal parliamentarians have called for removal; the Florida Surgeon General called for removal of all mRNA COVID-19 vaccines in

January 2024, citing cDNA fragment contamination and genotoxicity risk; and legal action seeking prohibition and withdrawal was filed in France in October 2024 [116].

The case for withdrawal does not rest on the concurrent-hit model alone. Independent lines of concern — excess mortality, absence of demonstrated reduction in transmission or mortality as primary endpoints, finished-product DNA contamination, and now a specified oncogenic risk architecture — converge on the same regulatory conclusion.

20. Conclusions

The nucleoside-modified mRNA–LNP platform presents a convergent oncogenic risk architecture that was not adequately characterized before mass deployment. 35 candidate mechanisms identified in the primary literature converge on four linked processes—protooncogene activation, mutation pressure, PPI-network rewiring, and CSC clonal acceleration—against a background of m1Ψ-dependent frameshifting, residual plasmid DNA and regulatory elements, multi-year product persistence, inflammatory LNP chemistry, and incompletely characterized long-horizon biodistribution [31]. These mechanisms include receptor-level protooncogene activation and TLR2-dependent invasion; p53 suppression by transfected spike DNA; APOBEC-driven somatic hypermutation and nuclear import associated with SV40 regulatory elements in residual plasmid DNA; integration-class events following lipid-based nucleic-acid delivery; RNA:DNA hybrids that shield spike-encoding DNA from nuclease clearance; frameshift products recoverable from human tissue; proteotoxic and ribosomal stress; inflammatory stem-cell imprinting; impaired immune surveillance; exhausted cytotoxic T cells in cancer patients; and interferon-driven awakening of dormant metastatic cells. No single mechanism carries the argument; the concurrence is the argument. Population-scale observations add a clinically relevant layer: the Italian province-wide cohort reported an adjusted cancer-hospitalization association of HR 1.23 with lag sensitivity, complementary Korean data reported associations across multiple solid tumors, and U.S. SEER data show a rise in early-onset cancer incidence during the period of mass mRNA deployment [85–87], and CDC WONDER mortality data show an inflection in US cancer deaths at the week of peak mRNA uptake, with published analysis reporting 154,330 excess cancer deaths since that point [106] and our own independent query of the same federal files placing the total between approximately 119,000 and 197,000 [107,109]. These observational findings are consistent with the model's central prediction of compressed time-to-progression, metastatic outgrowth, or clinical presentation in susceptible hosts.

The principal concern is therefore not necessarily uniform de novo cancer initiation in every recipient, but acceleration of existing oncogenic processes in susceptible individuals—particularly those with dormant micrometastases, residual disease, clonal hematopoiesis, DNA-repair vulnerability, prior malignancy, or stem-like tumor-cell reservoirs. These are also among the populations into which the same nucleoside-modified mRNA–LNP chassis is now being extended as neoantigen therapy, often after prior spike-mRNA exposure [77–79,82]. Spike was the first mass payload; changing the ORF does not erase the vehicle's unresolved liabilities. The unforeseen nature of frameshifting, residual regulatory DNA under LNP delivery, multi-year molecular persistence, and simultaneous occupancy of growth, repair, immune, and stemness pathways represents a major gap in pre-deployment characterization. Authorization programs were not designed to resolve accelerated cancer progression, metastatic competence, multi-year persistence, frameshift proteomics, lot-linked genomic effects, or off-target antigen expression. Continued broad exposure—and especially expansion into residual-cancer populations—therefore imposes unresolved risks that short-term immunogenicity, passive surveillance, and lipid-H-focused biodistribution cannot settle. That expansion has now sustained its first randomized failure. BNT122-01

tested an individualized mRNA neoantigen therapy as adjuvant monotherapy against watchful waiting in 327 patients with molecularly confirmed residual colorectal cancer—the exact host context identified above as highest-risk—and was terminated in August 2026 after crossing its futility boundary and, ten months later, generating a numerical overall survival imbalance between arms [90,91]. Given as monotherapy in the setting for which it was most rationally indicated, the approach did not outperform watchful waiting. The sponsor has not disclosed the direction or magnitude of the survival imbalance, and we do not infer it; we note that the endpoint most relevant to this review has been measured in a randomized trial and the result withheld. Two implications follow. The efficacy premise on which expansion into residual-disease populations was justified is now unsupported by its first controlled test. And because that test used uridine mRNA in a lipoplex rather than m1Ψ in ionizable LNP [92], it failed without the specific liabilities this review identifies—so there is no basis for expecting the m1Ψ–LNP chassis to rescue the strategy, and every reason under the concurrent-hit model to expect it to add risk to an approach that has not yet demonstrated benefit. On the combined weight of mechanism, structural liability, clinical observation, and population association, the authors call for immediate withdrawal of the nucleoside-modified mRNA–LNP platform from broad preventive use and suspension of its expanded use in adjuvant and neoadjuvant oncology pending independent resolution of these questions.

Laboratory, clinical, and population evidence align: the mechanisms predict that mRNA vaccines should accelerate cancer in susceptible people, published patient cases describe exactly that pattern, and national cancer registries record it at scale. These three lines of evidence share no common data source and no common failure mode, so the explanation that accounts for all three is exposure rather than bias. Given this convergence, the following actions are warranted: (1) immediately withdraw the nucleoside-modified mRNA–LNP platform from broad preventive use and suspend adjuvant/neoadjuvant oncology indications pending independent resolution of persistence, frameshift products, residual DNA, concurrent-hit molecular endpoints, biodistribution limitations, and lag-stratified cancer signals [31,85–88]; (2) record vaccine brand, dose number, date, and lot in tumor registries and oncology trials, with progression-free survival, metastasis-free survival, recurrence, and time-to-progression analyzed as exposure-stratified endpoints; (3) commission independent multi-omic studies comparing post-vaccination cancers with contemporaneous unvaccinated controls using ctDNA, RNA-seq, proteomics, PPI mapping, integration-site analysis, CSC markers, and invasion signatures linked to dose, lot, and lag; (4) mandate finished-product residual-DNA fragment profiling and frameshift-product surveillance and do not accept lipid-H clearance as evidence against persistence of free mRNA, residual DNA, frameshift products, or long-lived nucleic-acid species [31]; (5) pre-register concurrent-hit validation and falsification criteria before dedicated cohorts are unblinded; (6) integrate the Italian, Korean, and U.S. cancer signals into formal regulatory benefit–risk reassessment using lag-, infection-, dose-, and lot-stratified designs [85–87]; (7) prefer platforms that minimize residual regulatory DNA, frameshift-prone modified-mRNA architecture, uncontrolled systemic biodistribution, prolonged antigen expression, and chronic occupancy of EGFR–MYC–p53–stemness networks; (8) do not treat individualized informed consent as a substitute for resolution of a potentially platform-wide safety problem; (9) halt expansion of the same chassis into residual-disease oncology populations until its liabilities are independently resolved, because a better payload does not erase an imperfect vehicle and commercial urgency cannot substitute for long-horizon safety characterization; and (10) before further neoantigen or shared-antigen approvals, require direct evidence of where the encoded antigen is expressed through cassette-specific nucleic-acid mapping and MHC-I immunopeptidomics of myocardium, brain, endothelium, and other non-target tissues, together with prospective cardiac and neuronal injury-marker surveillance across the full dosing schedule [94–97].

Primum non nocere requires that unresolved platform-level liabilities be independently characterized before further population-scale or residual-cancer expansion.

Ethics Statement: Institutional Review Board approval and informed consent were not required for this study because it is a review based exclusively on previously published literature and publicly available sources. No human participants, animals, or identifiable personal data were involved.

Conflict of Interest Statement: John Catanzaro is the CEO and a shareholder of Neo7Bioscience.

Data Availability Statement: The mortality data analyzed in this review are publicly available from CDC WONDER (Provisional Mortality Statistics, 2018 through Last Week; Multiple Cause of Death, 1999-2020) and from CDC/NCHS Weekly Counts of Deaths by State and Select Causes, as cited. Query parameters are stated in the text and figure captions, and the derived series underlying Figure 9 are available from the corresponding author on request. All other data supporting the findings discussed herein are available in the cited published literature.

Funding Statement: No external funding was received for this project.

Acknowledgements: None

Generative AI statement: Artificial intelligence (AI) tools (ChatGPT) were used to assist in the generation and refinement of the figures included in this manuscript.

References

1. Hanahan D, Weinberg RA. Hallmarks of cancer: the next generation. Cell. 2011;144(5):646-674.doi:10.1016/j.cell.2011.02.013
2. Hanahan D. Hallmarks of cancer: new dimensions. Cancer Discov. 2022;12(1):31-46.doi:10.1158/2159-8290.CD-21-1059
3. Swanton C, Bernard E, Abbosh C, et al. Embracing cancer complexity: hallmarks of systemic disease. Cell. 2024;187(7):1589-1616.doi:10.1016/j.cell.2024.02.009
4. Vogelstein B, Papadopoulos N, Velculescu VE, Zhou S, Diaz LA Jr, Kinzler KW. Cancer genome landscapes. Science. 2013;339(6127):1546-1558.doi:10.1126/science.1235122
5. Sutherland JV, Bailar JC 3rd. The multihit model of carcinogenesis: etiologic implications for colon cancer. J Chronic Dis. 1984;37(6):465-480.doi:10.1016/0021-9681(84)90030-4
6. Zhao D, Ravikumar V, Leach TJ, et al. Inflammation-induced epigenetic imprinting regulates intestinal stem cells. Cell Stem Cell. 2024;31(10):1447-1464.e6.doi:10.1016/j.stem.2024.08.006
7. Bogen KT. Inflammation as a cancer co-initiator: new mechanistic model predicts low/negligible risk at noninflammatory carcinogen doses. Dose Response. 2019;17(2):1559325819847834.doi:10.1177/1559325819847834
8. Batlle E, Clevers H. Cancer stem cells revisited. Nat Med. 2017;23(10):1124-1134.doi:10.1038/nm.4409
9. Valdes Angues R, Perea Bustos Y. SARS-CoV-2 vaccination and the multi-hit hypothesis of oncogenesis. Cureus. 2023;15(12):e50703.doi:10.7759/cureus.50703
10. Catanzaro JA, Hulscher N, McCullough PA. Genomic integration and molecular dysregulation in aggressive stage IV bladder cancer following COVID-19 mRNA vaccination. Int J Innov Res Med Sci. 2025;10(10):380-386.doi:10.23958/ijirms/vol10-i10/2130
11. Seneff S, Nigh G, Kyriakopoulos AM, McCullough PA. Innate immune suppression by SARS-CoV-2 mRNA vaccinations. Food Chem Toxicol. 2022;164:113008.doi:10.1016/j.fct.2022.113008
12. Von Ranke NL, Zhang W, Anokhin P, et al. Synthetic messenger RNA vaccines and transcriptomic dysregulation: evidence from new-onset adverse events and cancers post-vaccination. World J Exp Med. 2025;15(4):113869.doi:10.5493/wjem.v15.i4.113869
13. Wrapp D, Wang N, Corbett KS, et al. Cryo-EM structure of the 2019-nCoV spike in the prefusion conformation. Science. 2020;367(6483):1260-1263.doi:10.1126/science.abb2507
14. Hsieh CL, Goldsmith JA, Schaub JM, et al. Structure-based design of prefusion-stabilized SARS-CoV-2 spikes. Science. 2020;369(6510):1501-1505.doi:10.1126/science.abd0826
15. Bangaru S, Ozorowski G, Turner HL, et al. Structural analysis of full-length SARS-CoV-2 spike protein from an advanced vaccine candidate. Science. 2020;370(6520):1089-1094.doi:10.1126/science.abe1502
16. Xia X. Detailed dissection and critical evaluation of the Pfizer/BioNTech and Moderna mRNA vaccines. Vaccines (Basel). 2021;9(7):734.doi:10.3390/vaccines9070734
17. Pallesen J, Wang N, Corbett KS, et al. Immunogenicity and structures of a rationally designed prefusion MERS-CoV spike antigen. Proc Natl Acad Sci U S A. 2017;114(35):E7348-E7357.doi:10.1073/pnas.1707304114
18. Heinz FX, Stiasny K. Distinguishing features of current COVID-19 vaccines: knowns and unknowns of antigen presentation and modes of action. NPJ Vaccines. 2021;6(1):104.doi:10.1038/s41541-021-00369-6
19. Corbett KS, Edwards DK, Leist SR, et al. SARS-CoV-2 mRNA vaccine design enabled by prototype pathogen preparedness. Nature. 2020;586(7830):567-571.doi:10.1038/s41586-020-2622-0
20. Walsh EE, Frenck RW Jr, Falsey AR, et al. Safety and immunogenicity of two RNA-based Covid-19 vaccine candidates. N Engl J Med. 2020;383(25):2439-2450.doi:10.1056/NEJMoa2027906
21. Hulscher N, Schmidt V, Mörz M, et al. Persistence of vaccine mRNA, plasmid DNA, spike protein, and genomic dysregulation over 3.5 years post-COVID-19 mRNA vaccination. Med Res Arch. 2026;14(6).doi:10.18103/mra.2026.0351
22. Yonker LM, Swank Z, Bartsch YC, et al. Circulating spike protein detected in post-COVID-19 mRNA vaccine myocarditis. Circulation. 2023;147(11):867-876.doi:10.1161/CIRCULATIONAHA.122.061025
23. Ogata AF, Cheng CA, Desjardins M, et al. Circulating severe acute respiratory syndrome coronavirus 2 (SARS-CoV-2) vaccine antigen detected in the plasma of mRNA-1273 vaccine recipients. Clin Infect Dis. 2022;74(4):715-718.doi:10.1093/cid/ciab465
24. Patterson BK, Yogendra R, Francisco EB, et al. Detection of S1 spike protein in CD16+ monocytes up to 245 days in SARS-CoV-2-negative post-COVID-19 vaccine syndrome (PCVS) individuals. Hum Vaccin Immunother. 2025;21(1):2494934.doi:10.1080/21645515.2025.2494934

25. Boros LG, Kyriakopoulos AM, Brogna C, Piscopo M, McCullough PA, Seneff S. Long-lasting, biochemically modified mRNA, and its frameshifted recombinant spike proteins in human tissues and circulation after COVID-19 vaccination. Pharmacol Res Perspect. 2024;12:e1218.doi:10.1002/prp2.1218

26. Bansal S, Perincheri S, Fleming T, et al. Cutting edge: circulating exosomes with COVID spike protein are induced by BNT162b2 (Pfizer-BioNTech) vaccination prior to development of antibodies: a novel mechanism for immune activation by mRNA vaccines. J Immunol. 2021;207(10):2405-2410.doi:10.4049/jimmunol.2100637

27. Speicher DJ, Rose J, McKernan K. Quantification of residual plasmid DNA and SV40 promoter-enhancer sequences in Pfizer/BioNTech and Moderna modRNA COVID-19 vaccines from Ontario, Canada. Autoimmunity. 2025;58:2551517.doi:10.1080/08916934.2025.2551517

28. König B, Kirchner JO. Methodological considerations regarding the quantification of DNA impurities in the COVID-19 vaccine Comirnaty. Methods Protoc. 2024;7(3):41.doi:10.3390/mps7030041

29. McKernan K, Helbert Y, Kane LT, McLaughlin S. Sequencing of bivalent Moderna and Pfizer mRNA vaccines reveals nanogram to microgram quantities of expression vector dsDNA per dose. Preprint. OSF Preprints. 2023. Accessed August 24, 2026.https://osf.io/b9t7m/

30. European Medicines Agency. Assessment of SV40 elements in the BNT162b2 plasmid. Accessed August 24, 2026.https://www.ema.europa.eu/en

31. Goody SMG, Rowbottom C, Liu Y, Chen N. Biodistribution of mRNA vaccines in rats: enrichment in injection site and lymph tissues and rapid clearance without tissue persistence. Mol Ther Nucleic Acids. 2026;37(2):102948.doi:10.1016/j.omtn.2026.102948

32. Irrgang P, Gerling J, Kocher K, et al. Class switch toward noninflammatory, spike-specific IgG4 antibodies after repeated SARS-CoV-2 mRNA vaccination. Sci Immunol. 2023;8:eade2798.doi:10.1126/sciimmunol.ade2798

33. Abue M, Mochizuki M, Shibuya-Takahashi R, et al. Repeated COVID-19 vaccination as a poor prognostic factor in pancreatic cancer: a retrospective, single-center cohort study. Cancers (Basel). 2025;17(12):2006.doi:10.3390/cancers17122006

34. Benitez Fuentes JD, Mohamed Mohamed K, de Luna Aguilar A, et al. Evidence of exhausted lymphocytes after the third anti-SARS-CoV-2 vaccine dose in cancer patients. Front Oncol. 2022;12:975980.doi:10.3389/fonc.2022.975980

35. Palakkott AR, Alneyadi A, Muhammad K, et al. The SARS-CoV-2 spike protein activates the epidermal growth factor receptor-mediated signaling. Vaccines (Basel). 2023;11(4):768.doi:10.3390/vaccines11040768

36. Suzuki YJ, Gychka SG. SARS-CoV-2 spike protein elicits cell signaling in human host cells: implications for possible consequences of COVID-19 vaccines. Vaccines (Basel). 2021;9(1):36.doi:10.3390/vaccines9010036

37. Isidoro C. SARS-CoV2 and anti-COVID-19 mRNA vaccines: is there a plausible mechanistic link with cancer? Cancers (Basel). 2025;17(23):3867.doi:10.3390/cancers17233867

38. Jahankhani K, Ahangari F, Adcock IM, Mortaz E. Possible cancer-causing capacity of COVID-19: is SARS-CoV-2 an oncogenic agent? Biochimie. 2023;213:130-138.doi:10.1016/j.biochi.2023.05.014

39. Jaiswal A, Shrivastav S, Kushwaha HR, Chaturvedi R, Singh RP. Oncogenic potential of SARS-CoV-2: targeting hallmarks of cancer pathways. Cell Commun Signal. 2024;22(1):447.doi:10.1186/s12964-024-01818-0

40. Lei Y, Zhang J, Schiavon CR, et al. SARS-CoV-2 spike protein impairs endothelial function via downregulation of ACE 2. Circ Res. 2021;128(9):1323-1326.doi:10.1161/CIRCRESAHA.121.318902

41. Gordon DE, Jang GM, Bouhaddou M, et al. A SARS-CoV-2 protein interaction map reveals targets for drug repurposing. Nature. 2020;583(7816):459-468.doi:10.1038/s41586-020-2286-9

42. Fiorini E, Malinova A, Schreyer D, et al. MYC ecDNA promotes intratumour heterogeneity and plasticity in PDAC. Nature. 2025;640(8060):811-819.doi:10.1038/s41586-025-08721-9

43. Jamieson CHM, Weissman IL. Stem-cell aging and pathways to precancer evolution. N Engl J Med. 2023;389(14):1310-1319.doi:10.1056/NEJMra2304431

44. Zhang S, El-Deiry WS. Transfected SARS-CoV-2 spike DNA for mammalian cell expression inhibits p53 activation of p21(WAF1), TRAIL death receptor DR5 and MDM2 proteins in cancer cells and increases cancer cell viability after chemotherapy exposure. Oncotarget. 2024;15:275-284.doi:10.18632/oncotarget.28582

45. Aldén M, Olofsson Falla F, Yang D, et al. Intracellular reverse transcription of Pfizer BioNTech COVID-19 mRNA vaccine BNT162b2 in vitro in human liver cell line. Curr Issues Mol Biol. 2022;44(3):1115-1126.doi:10.3390/cimb44030073

46. Zhang L, Richards A, Barrasa MI, Hughes SH, Young RA, Jaenisch R. Reverse-transcribed SARS-CoV-2 RNA can integrate into the genome of cultured human cells and can be expressed in patient-derived tissues. Proc Natl Acad Sci U S A. 2021;118(21):e2105968118.doi:10.1073/pnas.2105968118

47. Lim S, Yocum RR, Silver PA, Way JC. High spontaneous integration rates of end-modified linear DNAs upon mammalian cell transfection. Sci Rep. 2023;13(1):6835.doi:10.1038/s41598-023-33862-0

48. Mulroney TE, Poyry T, Yam-Puc JC, et al. N1-methylpseudouridylation of mRNA causes +1 ribosomal frameshifting. Nature. 2024;625(7993):189-194.doi:10.1038/s41586-023-06800-3

49. Ndeupen S, Qin Z, Jacobsen S, Bouteau A, Estanbouli H, Igyártó BZ. The mRNA-LNP platform's lipid nanoparticle component used in preclinical vaccine studies is highly inflammatory. iScience. 2021;24(12):103479.doi:10.1016/j.isci.2021.103479

50. Šenigl F, Soikkeli AI, Prost S, et al. The SV40 virus enhancer functions as a somatic hypermutation-targeting element with potential tumorigenic activity. Tumour Virus Res. 2024;18:200293.doi:10.1016/j.tvr.2024.200293

51. Dean DA, Strong DD, Zimmer WE. Nuclear entry of nonviral vectors. Gene Ther. 2005;12:881-890.doi:10.1038/sj.gt.3302534

52. Strayer D, Branco F, Zern MA, et al. Durability of transgene expression and vector integration: recombinant SV40-derived gene therapy vectors. Mol Ther. 2002;6:227-237.doi:10.1006/mthe.2002.0657

53. Lemp NA, Hiraoka K, Kasahara N, Logg CR. Cryptic transcripts from a ubiquitous plasmid origin of replication confound tests for cis-regulatory function. Nucleic Acids Res. 2012;40:7280-7290.doi:10.1093/nar/gks451

54. Drayman N, Ben-Nun-Shaul O, Butin-Israeli V, et al. p53 elevation in human cells halt SV40 infection by inhibiting T-ag expression. Oncotarget. 2016;7:52643-52660.doi:10.18632/oncotarget.10769

55. Fu H, Mo X, Ivanov AA. Decoding the functional impact of the cancer genome through protein-protein interactions. Nat Rev Cancer. 2025;25(3):189-208.doi:10.1038/s41568-024-00784-6

56. Kennedy SA, Jarboui MA, Srihari S, et al. Extensive rewiring of the EGFR network in colorectal cancer cells expressing transforming levels of KRAS(G13D). Nat Commun. 2020;11(1):499.doi:10.1038/s41467-019-14224-9

57. Agudo J, Miao Y. Stemness in solid malignancies: coping with immune attack. Nat Rev Cancer. 2025;25(1):27-40.doi:10.1038/s41568-024-00760-0

58. Du J, Xu Y, Sasada S, et al. Signaling inhibitors accelerate the conversion of mouse iPS cells into cancer stem cells in the tumor microenvironment. Sci Rep. 2020;10(1):9955.doi:10.1038/s41598-020-66471-2

59. Chia SB, Johnson BJ, Hu J, et al. Respiratory viral infections awaken metastatic breast cancer cells in lungs. Nature. 2025;645:496-506.doi:10.1038/s41586-025-09332-0

60. Wang B, Hao Y, Hong W, et al. Lipid nanoparticle used in mRNA vaccine promotes tumor metastasis in mouse model via mtDNA-induced neutrophil activation and NETosis. Nano Today. 2026;69:103039.doi:10.1016/j.nantod.2026.103039

61. Gregory TA, Knight SR, Aaroe AE, et al. Accelerated tumor progression after COVID-19 infection in patients with glioblastoma: a retrospective case-control study. Neurooncol Pract. 2024;11:475-483.doi:10.1093/nop/npae029

62. US Food and Drug Administration. FDA response on residual DNA and genotoxicity. 2023. Accessed August 24, 2026.https://www.fda.gov/media/174875/download

63. Nance KD, Meier JL. Modifications in an emergency: the role of N1-methylpseudouridine in COVID-19 vaccines. ACS Cent Sci. 2021;7(5):748-756.doi:10.1021/acscentsci.1c00197

64. Karikó K, Muramatsu H, Welsh FA, et al. Incorporation of pseudouridine into mRNA yields superior nonimmunogenic vector with increased translational capacity and biological stability. Mol Ther. 2008;16(11):1833-1840.doi:10.1038/mt.2008.200

65. Tursi NJ, Weiner DB. Modified messenger-RNA components alter the encoded protein. Nature. 2024;625(7993):37-38.doi:10.1038/d41586-023-03787-9

66. Zhang H, Zhang L, Lin A, et al. Algorithm for optimized mRNA design improves stability and immunogenicity. Nature. 2023;621(7978):396-403.doi:10.1038/s41586-023-06127-z

67. Achs A, Sedlackova T, Predajna L, et al. Systematic analysis of COVID-19 mRNA vaccines using four orthogonal approaches demonstrates no excessive DNA impurities. NPJ Vaccines. 2025;10:259.doi:10.1038/s41541-025-01304-9

68. McKernan K, Speicher DJ, Rose J. Systematic methodological flaws in DNA contamination assessment of mRNA vaccines: a critical analysis of Achs et al. (2025). Oncotarget. 2026;17(1):368-376.doi:10.18632/oncotarget.28913

69. Sutton DH, Conn GL, Brown T, Lane AN. The dependence of DNase I activity on the conformation of oligodeoxynucleotides. Biochem J. 1997;321:481-486.doi:10.1042/bj3210481

70. Lenk R, Kleindienst W, Szabó GT, et al. Understanding the impact of in vitro transcription byproducts and contaminants. Front Mol Biosci. 2024;11:1426129.doi:10.3389/fmolb.2024.1426129

71. McKernan K, Rixey J, Rose J. RNA:DNA hybrids in mRNA vaccines resist nuclease digestion and protect spike-encoding sequences. Preprint. Zenodo. 2024. Accessed August 24, 2026.https://zenodo.org/records/17832183

72. Issa WJ, Wang Y, Bancel S; ModernaTx, Inc. Removal of DNA fragments in mRNA production process. US patent 10,077,439 B2. September 18, 2018. Accessed August 24, 2026.https://patents.google.com/patent/US10077439B2/en

73. de Fougerolles A, Elbashir SM; ModernaTx, Inc. Delivery and formulation of engineered nucleic acids. US patent 10,898,574 B2. January 26, 2021. Accessed August 24, 2026.https://patents.google.com/patent/US10898574B2/en

74. Grippin AJ, Marconi C, Copling S, et al. SARS-CoV-2 mRNA vaccines sensitize tumours to immune checkpoint blockade. Nature. 2025;647(8089):488-497.doi:10.1038/s41586-025-09655-y

75. Wilson E, Goswami J, Baqui AH, et al. Efficacy and safety of an mRNA-based RSV PreF vaccine in older adults. N Engl J Med. 2023;389(24):2233-2244.doi:10.1056/NEJMoa2307079

76. Moderna, Inc. US FDA approval of mFLUSIVA (mRNA-1010), Moderna's seasonal influenza vaccine. 2026. Accessed August 28, 2026.https://www.modernatx.com/ir-insights-mflusiva

77. Moderna, Merck. mRNA-4157 (intismeran autogene) phase 3 melanoma program disclosures. Nature. 2026. Accessed August 24, 2026.https://www.nature.com/articles/d41586-026-02612-3

78. Weber JS, Carlino MS, Khattak A, et al. Individualised neoantigen therapy mRNA-4157 (V940) plus pembrolizumab versus pembrolizumab monotherapy in resected melanoma (KEYNOTE-942): a randomised, phase 2b study. Lancet. 2024;403(10427):632-644.doi:10.1016/S0140-6736(23)02268-7

79. Moderna, Inc. Form 10-K: pipeline description of intismeran autogene manufacturing and LNP formulation. US Securities and Exchange Commission. Accessed August 24, 2026.https://edgar.secdatabase.com/1959/168285226000033/filing-main.htm

80. ASCO 2026 mRNA tumor vaccine antigens: competitive landscape analysis. PatSnap Eureka. 2026. Accessed August 24, 2026.https://eureka.patsnap.com/blog/life-science/asco-2026-mrna-tumor-vaccine-antigens-competitive-landscape-analysis/

81. Moderna Science Day highlights expanding potential of mRNA platform: mRNA-4106, mRNA-4200, mRNA-4194, and mRNA-4359 oncology assets. Nasdaq. June 25, 2026. Accessed August 24, 2026.https://www.nasdaq.com/press-release/moderna-science-day-highlights-expanding-potential-mrna-platform-2026-06-25

82. Merck, Moderna. Intismeran autogene manufacturing and LNP similarity to Spikevax; nine doses every three weeks. SMR 2025 poster P168. Accessed August 24, 2026.https://irp.cdn-website.com/89dd0539/files/uploaded/P168_SMR+2025_End-to-End+Poster+%282%29.pdf

83. Merck and Moderna announce phase 3 INTerpath-001 trial of intismeran autogene plus KEYTRUDA met endpoints of recurrence-free survival and distant metastasis-free survival. Merck. 2026. Accessed August 24, 2026.https://www.merck.com/news/merck-and-moderna-announce-phase-3-interpath-001-trial-of-intismeran-autogene-plus-keytruda-met-endpoints-of-recurrence-free-survival-rfs-and-distant-metastasis-free-survival-dmfs-in-patient/

84. McCullough PA. The mRNA gold rush: why Moderna's “cancer vaccine” hype will get challenged. Focal Points. August 24, 2026. Accessed August 24, 2026.https://www.thefocalpoints.com/p/the-mrna-gold-rush-why-modernas-cancer

85. Acuti Martellucci C, Capodici A, Soldato G, et al. COVID-19 vaccination, all-cause mortality, and hospitalization for cancer: 30-month cohort study in an Italian province. EXCLI J. 2025;24:690-707.doi:10.17179/excli2025-8400

86. Kim HJ, Kim MH, Choi MG, Chun EM. One-year risks of cancers associated with COVID-19 vaccination: a large population-based cohort study in South Korea. Biomark Res. 2025;13(1):114.doi:10.1186/s40364-025-00831-w

87. National Cancer Institute, Surveillance, Epidemiology, and End Results Program. SEER*Explorer: an interactive website for SEER cancer statistics. SEER Incidence Data, November 2025 Submission (1975-2023), SEER 21 registries. Accessed September 2, 2026.https://seer.cancer.gov/statistics-network/explorer/

88. Debord M. Les vaccins ARNm anti-COVID peuvent induire le cancer de 17 manières distinctes selon plus de 100 études. Le Point Critique. June 19, 2025. Accessed August 24, 2026.https://lepointcritique.fr/2025/06/19/vaccins-arnm-anti-covid-peuvent-induire-cancer-de-17-manieres-distinctes-selon-plus-de-100-etudes/

89. Roy O, Anderson KS. Engineering anti-tumor immunity: an immunological framework for mRNA cancer vaccines. Vaccines (Basel). 2025;13(12):1222.doi:10.3390/vaccines13121222

90. BioNTech SE. BioNTech provides update on Phase 2 clinical trial of autogene cevumeran in resected colorectal cancer. Published August 28, 2026. Accessed August 31, 2026.https://www.biontech.com/int/en/home/mediaroom/news/statements/2026/08/BioNTech-Provides-Update-on-Phase-2-Clinical-Trial-of-Autogene-Cevumeran-in-Resected-Colorectal-Cancer.html

91. BioNTech SE. A study of autogene cevumeran versus watchful waiting in patients with circulating tumor DNA-positive, resected stage II (high risk) and stage III colorectal cancer (BNT122-01). ClinicalTrials.gov identifier: NCT04486378. Accessed August 31, 2026.https://clinicaltrials.gov/study/NCT04486378

92. Lang F, Kušnierczyk P, Vormehr M, et al. Characterization of T cell responses induced by the individualized mRNA neoantigen vaccine autogene cevumeran in adjuvant stage II (high risk)/stage III colorectal cancer patients from the biomarker cohort of the phase II BNT122-01 trial. Ann Oncol. 2024;35(suppl 1):S13.doi:10.1016/j.annonc.2024.02.043

93. Krauson AJ, Casimero FVC, Siddiquee Z, Stone JR. Duration of SARS-CoV-2 mRNA vaccine persistence and factors associated with cardiac involvement in recently vaccinated patients. NPJ Vaccines. 2023;8(1):141.doi:10.1038/s41541-023-00742-7

94. Linette GP, Stadtmauer EA, Maus MV, et al. Cardiovascular toxicity and titin cross-reactivity of affinity-enhanced T cells in myeloma and melanoma. Blood. 2013;122(6):863-871.doi:10.1182/blood-2013-03-490565

95. Cameron BJ, Gerry AB, Dukes J, et al. Identification of a Titin-derived HLA-A1-presented peptide as a cross-reactive target for engineered MAGE A3-directed T cells. Sci Transl Med. 2013;5(197):197ra103.doi:10.1126/scitranslmed.3006034

96. Morgan RA, Chinnasamy N, Abate-Daga D, et al. Cancer regression and neurological toxicity following anti-MAGE-A3 TCR gene therapy. J Immunother. 2013;36(2):133-151.doi:10.1097/CJI.0b013e3182829903

97. Morgan RA, Yang JC, Kitano M, Dudley ME, Laurencot CM, Rosenberg SA. Case report of a serious adverse event following the administration of T cells transduced with a chimeric antigen receptor recognizing ERBB2. Mol Ther. 2010;18(4):843-851.doi:10.1038/mt.2010.24

98. Bergmann O, Bhardwaj RD, Bernard S, et al. Evidence for cardiomyocyte renewal in humans. Science. 2009;324(5923):98-102.doi:10.1126/science.1164680

99. Mitrofanova L, Makarov I, Goncharova E, et al. High risk of heart tumors after COVID-19. Life (Basel). 2023;13(10):2087.doi:10.3390/life13102087

100. Schreckenberg R, Woitasky N, Itani N, Czech L, Ferdinandy P, Schulz R. Cardiac side effects of RNA-based SARS-CoV-2 vaccines: hidden cardiotoxic effects of mRNA-1273 and BNT162b2 on ventricular myocyte function and structure. Br J Pharmacol. 2024;181(3):345-361.doi:10.1111/bph.16262

101. Salem JE, Manouchehri A, Moey M, et al. Cardiovascular toxicities associated with immune checkpoint inhibitors: an observational, retrospective, pharmacovigilance study. Lancet Oncol. 2018;19(12):1579-1589.doi:10.1016/S1470-2045(18)30608-9

102. Ota N, Itani M, Aoki T, et al. Expression of SARS-CoV-2 spike protein in cerebral arteries: implications for hemorrhagic stroke post-mRNA vaccination. J Clin Neurosci. 2025;136:111223.doi:10.1016/j.jocn.2025.111223

103. Locquet M, Beaudart C, Douxfils J, Roberfroid D, Van Damme P, Dogné JM. Commentary: 1-year risks of cancers associated with COVID-19 vaccination: a large population-based cohort study in South Korea. Front Public Health. 2026;14:1772406.doi:10.3389/fpubh.2026.1772406

104. Kuperwasser C, El-Deiry WS. COVID vaccination and post-infection cancer signals: evaluating patterns and potential biological mechanisms. Oncotarget. 2026;17:1-29.doi:10.18632/oncotarget.28824

105. Russell SJ, Mabila SL. Non-Hodgkin lymphoma incidence in active component U.S. service members, 2017-2023. MSMR. 2025;32:16-17.

106. The Ethical Skeptic. The state of things pandemic — week 13 2026. Published March 13, 2026. Accessed August 24, 2026.https://theethicalskeptic.com/2026/03/13/the-state-of-things-pandemic/

107. Centers for Disease Control and Prevention, National Center for Health Statistics. National Vital Statistics System, Provisional Mortality on CDC WONDER Online Database. Underlying cause of death, malignant neoplasms (C00-C97), grouped by month. Data are from the final Multiple Cause of Death Files, 2018-2024, and from provisional data for years 2025 and later. Accessed September 2, 2026.http://wonder.cdc.gov/mcd-icd10-provisional.html

108. Centers for Disease Control and Prevention, National Center for Health Statistics. Weekly counts of deaths by state and select causes, 2014-2019 and 2020-2023. National Vital Statistics System. Accessed September 2, 2026.https://data.cdc.gov/NCHS/Weekly-Counts-of-Deaths-by-State-and-Select-Causes/3yf8-kanr

109. Centers for Disease Control and Prevention, National Center for Health Statistics. National Vital Statistics System, Multiple Cause of Death on CDC WONDER Online Database. Malignant neoplasms (C00-C97) recorded as any cause on the death certificate, grouped by month; final file 1999-2020 and provisional file 2018 onward. Accessed September 2, 2026. http://wonder.cdc.gov/mcd.html

110. Sano S. A case of metastatic breast carcinoma to the skin expressing SARS-CoV-2 spike protein possibly derived from mRNA vaccine. J Dermatol Sci. 2025;120:71-73.doi:10.1016/j.jdermsci.2025.09.007

111. Kim MJ, Kim JY, Shin JH, et al. The SARS-CoV-2 spike protein induces lung cancer migration and invasion in a TLR2-dependent manner. Cancer Commun (Lond). 2024;44(2):273-277.doi:10.1002/cac2.12485

112. Li H, Wan L, Liu M, et al. SARS-CoV-2 spike-induced syncytia are senescent and contribute to exacerbated heart failure. PLoS Pathog. 2024;20(6):e1012291.doi:10.1371/journal.ppat.1012291

113. Moutal A, Martin LF, Boinon L, et al. SARS-CoV-2 spike protein co-opts VEGF-A/neuropilin-1 receptor signaling to induce analgesia. Pain. 2021;162(1):243-252.doi:10.1097/j.pain.0000000000002097

114. Kwon J, Bakhoum SF. The cytosolic DNA-sensing cGAS-STING pathway in cancer. Cancer Discov. 2020;10(1):26-39.doi:10.1158/2159-8290.CD-19-0761

115. Bhattacharjee B, Lu P, Monteiro VS, et al. Immunological and antigenic signatures associated with chronic illnesses after COVID-19 vaccination. Preprint. medRxiv. 2025.doi:10.1101/2025.02.18.25322379

116. Hulscher N, Bowden MT, McCullough PA. Review: calls for market removal of COVID-19 vaccines intensify as risks far outweigh theoretical benefits. Sci Public Health Policy Law. 2025;6:2019-2025. Accessed August 25, 2026.https://publichealthpolicyjournal.com/